



**NEUTRONIC INVESTIGATION OF THE EFFECT  
OF FIRST WALL MATERIAL COMPOSITION  
AND THICKNESS ON REACTOR STRUCTURE  
PERFORMANCE IN A FUSION REACTOR**

**2022**

**PhD THESIS  
ENERGY SYSTEMS ENGINEERING**

**MELOOD MOHAMAD OMAR TAJOORE**

**Thesis Advisor  
Prof. Dr. Hacı Mehmet ŞAHİN**

**NEUTRONIC INVESTIGATION OF THE EFFECT OF FIRST WALL  
MATERIAL COMPOSITION AND THICKNESS ON REACTOR  
STRUCTURE PERFORMANCE IN A FUSION REACTOR**

**Melood Mohamad OMAR TAJOORE**

**T.C.  
Karabuk University  
Institute of Graduate Programs  
Department of Energy Systems Engineering  
Prepared as  
PhD Thesis**

**Thesis Advisor  
Prof. Dr. Hacı Mehmet ŞAHİN**

**KARABUK  
July 2022**

I certify that in my opinion the thesis submitted by Melood Mohamad OMAR TAJOORE titled “NEUTRONIC INVESTIGATION OF THE EFFECT OF FIRST WALL MATERIAL COMPOSITION AND THICKNESS ON REACTOR STRUCTURE PERFORMANCE IN A FUSION REACTOR” is fully adequate in scope and in quality as a thesis for the degree of PhD.

Prof. Dr. Hacı Mehmet ŞAHİN .....

Thesis Advisor, Department of Energy Systems Engineering

This thesis is accepted by the examining committee with a unanimous vote in the Department of Energy Systems Engineering as a PhD thesis. July 19, 2022

Examining Committee Members (Institutions)

Signature

Chairman : Prof. Dr. Mehmet ÖZKAYMAK (KBU) .....

Member : Prof. Dr. Hacı Mehmet ŞAHİN (KBU) .....

Member : Prof. Dr. Mustafa AKTAŞ (GU) .....

Member : Assoc. Prof. Dr. Engin GEDİK (KBU) .....

Member : Assist. Prof. Dr. Güven TUNÇ (GU) .....

The degree of PhD by the thesis submitted is approved by the Administrative Board of the Institute of Graduate Programs, Karabuk University.

Prof. Dr. Hasan SOLMAZ .....

Director of the Institute of Graduate Programs



*“I declare that all the information within this thesis has been gathered and presented in accordance with academic regulations and ethical principles and I have according to the requirements of these regulations and principles cited all those which do not originate in this work as well.”*

Melood Mohamad OMAR TAJOORE

## **ABSTRACT**

**PhD Thesis**

### **NEUTRONIC INVESTIGATION OF THE EFFECT OF FIRST WALL MATERIAL COMPOSITION AND THICKNESS ON REACTOR STRUCTURE PERFORMANCE IN A FUSION REACTOR**

**Melood Mohamad OMAR TAJOORE**

**Karabük University**

**Institute of Graduate Programs**

**The Department of Energy Systems Engineering**

**Thesis Advisor:**

**Prof. Dr. Hacı Mehmet ŞAHİN**

**July 2022, 54 pages**

In this study, the effects of changing first wall materials and their thickness on the reactor were investigated displacement per atom (DPA) and gas production (He and H) in the first wall and tritium breeding ratio (TBR) in the coolant zone and the tritium breeding zone. Therefore, the modeling of a magnetic fusion reactor was determined based on the blanket parameters of the International Thermonuclear Experimental Reactor (ITER). Stainless Steel (SS 316 LN-IG), Oxide Dispersion Strengthened Steel Alloy (PM2000 ODS) and China low activation martensitic steel (CLAM) were used as a First Wall (FW) materials. Fluorides family molten salt materials (FLiBe, FLiNaBe, FLiPb) and Lithium oxide (LiO<sub>2</sub>) were considered as a coolant and the tritium production material in the blanket, respectively. Neutron transport calculations were performed by the well-known 3D code MCNP5 using the continuous energy Monte Carlo methods. It uses the latest built-in continuous energy nuclear and atomic

data libraries, the Evaluated Nuclear Data File (ENDF) system (ENDF/B-V and ENDF/B-VI). Additionally, the activity cross section data library CLAW-IV was considered to evaluate both DPA values and gas production of first wall (FW) materials. The interface computer program written in FORTRAN 90 language to evaluate the MCNP5 outputs was developed for the fusion reactor blanket. The results concluded that the best TBR value was obtained for the use of FLiPb coolant, while the first wall replacement period in terms of radiation damage to all materials was between 6 and 11 years depending on the thickness.

**Key Words** : ITER, First wall material, Material damage, Tritium breeding ratio, Fluorides family molten salt materials.

**Science Code** : 92805

## ÖZET

Doktora Tezi

### BİR FÜZYON REAKTÖRÜNDE İLK DUVAR MALZEME BİLEŞİMİ VE KALINLIĞININ REAKTÖR YAPI PERFORMANSINA ETKİSİNİN NÖTRONİK İNCELENMESİ

Melood Mohamad OMAR TAJOORE

Karabük Üniversitesi

Lisansüstü Eğitim Enstitüsü

Enerji Sistemleri Mühendisliği Anabilim Dalı

Tez Danışmanı:

Prof. Dr. Hacı Mehmet ŞAHİN

Temmuz 2022, 54 sayfa

Bu çalışmada, değişen birinci duvar malzemelerinin ve kalınlıklarının reaktör üzerindeki etkileri, birinci duvarda atom başına yer değiştirme (DPA) ve gaz üretimi (He ve H) soğutucu akışkan ve trityum üreme bölgelerindeki trityum üretim oranı (TBR) araştırılmıştır. Bu nedenle, bir manyetik füzyon reaktörünün modellenmesi, Uluslararası Termonükleer Deneysel Reaktörün (ITER) battaniye parametrelerine bağlı olarak belirlenmiştir. Birinci Duvar (FW) malzemeleri olarak Paslanmaz Çelik (SS 316LN-IG), Oksit Dağılımla Güçlendirilmiş Çelik Alaşımı (PM2000 ODS) ve Çin Düşük Aktivasyonlu Martensitik Çelik (CLAM) kullanıldı. Florür ailesi erimiş tuz malzemeleri (FLiBe, FLiNaBe, FLiPb) ve Lityum oksit (LiO<sub>2</sub>), battaniyede sırasıyla bir soğutucu ve trityum üretim malzemesi olarak ele alınmıştır. Nötron transport hesaplamaları, sürekli enerji şartlarında Monte Carlo yöntemi kullanılarak 3 Boyutlu kod olan MCNP5 ile yapılmıştır. Sürekli enerjili nükleer ve atomik veri kütüphaneleri

olan, Evaluated Nuclear Data File (ENDF) sistemi (ENDF/B-V ve ENDF/B-VI) kullanılmıştır. Ayrıca, birinci duvar (FW) malzemelerinin hem DPA değerlerini hem de gaz üretimini değerlendirmek için CLAW-IV tesir kesit kütüphanesi kullanılmıştır. Füzyon reaktörü battaniyesinde MCNP5 çıktıları değerlendirilmek için FORTRAN 90 dilinde yazılmış arayüz bilgisayar programı geliştirilmiştir. Sonuçlar, en iyi TBR değerinin FLiPb soğutucu kullanımı için elde edildiği, tüm malzemelerde radyasyon hasarı açısından ilk duvar değiştirme süresinin kalınlığa bağlı olarak 6 ila 11 yıl arasında olduğu sonucuna varmıştır.

**Anahtar Kelimeler :** ITER, Birinci duvar malzemesi, Malzeme hasarı, Tritiyum üretim oranı, Florür ailesi, Erimiş tuz malzemeleri.

**Bilim Kodu :** 92805

## **ACKNOWLEDGEMENT**

I would like to express my special thanks to my supervisor of the thesis Prof. Dr. Haci Mehmet Şahin, for his attention, patience, guidance and assistance in preparing a thesis throughout the study period. I would also like to thank a head department of Energy Systems, Prof. Dr, Mehmet Özkaymak and all the staff members of the department.



## CONTENTS

|   | <u>Page</u> |
|---|-------------|
| APPROVAL.....   | ii          |
| ABSTRACT.....   | iv          |
| ÖZET.....   | vi          |
| ACKNOWLEDGEMENT .....   | viii        |
| CONTENTS.....   | ix          |
| LIST OF FIGURES .....   | xi          |
| LIST OF TABLES .....  | xiii        |
| SYMBOLS AND ABBREVIATIONS INDEX .....                                     | xiv         |
| <br>  |             |
| CHAPTER 1 .....   | 1           |
| INTRODUCTION .....  | 1           |
| 1.1. BACKGROUND.....  | 1           |
| 1.2. NUCLEAR FUSION.....  | 4           |
| 1.3. FUSION IN STARS.....   | 6           |
| 1.4. APPLICATION OF FUSION IN ENERGY PRODUCTION.....                      | 7           |
| 1.4.1. Conditions For Fusion .....  | 7           |
| 1.4.2. Confinement Time .....   | 8           |
| 1.4.3. Ion Density.....   | 8           |
| 1.4.4. Fusion Reactors .....  | 9           |
| 1.5. AIMS AND OBJECTIVES.....   | 9           |
| <br>  |             |
| CHAPTER 2 .....   | 11          |
| LITERATURE OVERVIEW.....  | 11          |
| <br>  |             |
| CHAPTER 3 .....   | 15          |
| METHOD.....   | 15          |
| 3.1. DESCRIPTION OF GEOMETRICAL MODEL FOR NEUTRONIC<br>CALCULATIONS ..... | 15          |
| 3.2. NEUTRON TRANSPORT EQUATION.....                                      | 21          |
| 3.2.1. Particle Transport Equation .....                                  | 21          |

|  | <u>Page</u> |
|--|-------------|
| 3.2.2. MCNP and Interface Code Structure ..... | 22          |
| 3.3. CALCULATION TOOLS.....                    | 22          |
| CHAPTER 4 .....                                | 25          |
| RESULTS AND DISCUSSION .....                   | 25          |
| 4.1. FUSION BLANKET PERFORMANCE .....          | 25          |
| 4.1.1. Tritium Breeding Ratio.....             | 25          |
| 4.1.2. Energy Multiplication Factor.....       | 31          |
| 4.2. RADIATION DAMAGE IN THE FIRST WALL.....   | 32          |
| 4.2.1. Displacement Per Atom.....              | 34          |
| 4.2.2. Gas Production.....                     | 35          |
| 4.2.3. Structural Lifetime.....                | 42          |
| CHAPTER 5 .....                                | 47          |
| CONCLUSIONS AND FUTURE WORK .....              | 47          |
| 5.1. CONCLUSIONS .....                         | 47          |
| 5.2. FUTURE WORKS .....                        | 49          |
| REFERENCES.....                                | 50          |
| RESUME .....                                   | 54          |

## LIST OF FIGURES

|   | <u>Page</u> |
|---|-------------|
| Figure 1.1. A typical nuclear fusion reaction. ....   | 5           |
| Figure 1.2. D-D and D-T nuclear fusion reaction. ....   | 5           |
| Figure 1.3. Fusion in stars .....   | 6           |
| Figure 1.4. Energy released at each step. ....  | 7           |
| Figure 1.5. Magnetic confinement reactor .....  | 9           |
| Figure 3.1. Blanket structure of investigated magnetic fusion reactor.....  | 16          |
| Figure 3.2. Flowchart of the problem solution.....  | 24          |
| Figure 4.1. Cross Section of Be(n,2n) and Pb(n,2n) at the KAERI Nuclear Data Center.....  | 26          |
| Figure 4.2. The coolants neutron spectrum at coolant region (with 5 cm SS316LN-IG First wall Thickness) .....   | 27          |
| Figure 4.3. The Change of Tritium Breeding Ratio with respect to Thickness for SS 316 LN-IG Steel Alloy First Wall Material (given separately in the coolant zone and the tritium breeding zone)..... | 28          |
| Figure 4.4. The Change of Tritium Breeding Ratio with respect to Thickness for PM2000 ODS Steel Alloy First Wall Materials (given separately in the coolant zone and the tritium breeding zone).....  | 28          |
| Figure 4.5. The Change in Tritium Breeding Ratio with respect to Thickness for CLAM Steel Alloy First Wall Materials (given separately in the coolant zone and the tritium breeding zone). ....       | 29          |
| Figure 4.6. The Change in the Tritium Breeding Ratio with respect to Thickness for SS 316 LN-IG Steel Alloy First Wall Materials. ....  | 30          |
| Figure 4.7. The Change in the Tritium Breeding Ratio with respect to Thickness for PM2000 ODS Steel Alloy First Wall Materials. ....  | 30          |
| Figure 4.8. The Change in the Tritium Breeding Ratio with respect to Thickness for CLAM Steel Alloy First Wall Materials.....   | 31          |
| Figure 4.9. The Change in the Multiplication Factor with respect to Thickness for SS 316 LN-IG Steel Alloy First Wall Materials and Coolants.....   | 32          |
| Figure 4.10. The Change in the Multiplication Factor with respect to Thickness for PM2000 ODS Steel Alloy First Wall Materials and Coolants .....   | 33          |
| Figure 4.11. The Change in the Multiplication Factor with respect to Thickness for CLAM Steel Alloy First Wall Materials and Coolants.....  | 33          |
| Figure 4.12. The Change in the Displacement per Atom with respect to Thickness for SS 316 LN-IG Steel Alloy First Wall Materials. ....  | 36          |

|   | <u>Page</u> |
|---|-------------|
| Figure 4.13. The Change in the Displacement per Atom with respect to Thickness for PM2000 ODS Steel Alloy First Wall Materials.....                     | 36          |
| Figure 4.14. The Change in the Displacement per Atom with respect to Thickness for CLAM Steel Alloy First Wall Materials. ....                          | 37          |
| Figure 4.15. The Change in Hydrogen Production with respect to Thickness for SS 316 LN-IG Steel Alloy First Wall Materials. ....                        | 38          |
| Figure 4.16. The Change in Hydrogen Production with respect to Thickness for PM2000 ODS Steel Alloy First Wall Materials. ....                          | 38          |
| Figure 4.17. The Change in Hydrogen Production with respect to Thickness for CLAM Steel Alloy First Wall Materials.....                                 | 39          |
| Figure 4.18. The Change in Helium Production with respect to Thickness for SS 316 LN-IG Steel Alloy First Wall Materials. ....                          | 40          |
| Figure 4.19. The Change in Helium Production with respect to Thickness for PM2000 ODS Steel Alloy First Wall Materials. ....                            | 40          |
| Figure 4.20. The Change in Helium Production with respect to Thickness for CLAM Steel Alloy First Wall Materials.....                                   | 41          |
| Figure 4.21. The Change in Structural Lifetime with respect to Thickness for SS 316 LN-IG Steel Alloy First Wall Materials Regarding the DPA Limit..... | 41          |
| Figure 4.22. The Change in Structural Lifetime with respect to Thickness for PM2000 ODS Steel Alloy First Wall Materials Regarding the DPA Limit.....   | 43          |
| Figure 4.23. The Change in Structural Lifetime with respect to Thickness for CLAM Steel Alloy First Wall Materials Regarding the DPA Limit. ...         | 43          |
| Figure 4.24. The Change in Structural Lifetime with respect to Thickness for SS 316 LN-IG Steel Alloy First Wall Materials Regarding He Limit. ....     | 44          |
| Figure 4.25. The Change in Structural Lifetime with respect to Thickness for PM2000 ODS Steel Alloy First Wall Materials Regarding He Limit. .          | 45          |
| Figure 4.26. The Change in Structural Lifetime with respect to Thickness for CLAM Steel Alloy First Wall Materials Regarding He Limit. ....             | 45          |

## LIST OF TABLES

|  | <b><u>Page</u></b> |
|--|--------------------|
| Table 3.1. Atomic densities of the blanket materials .....   | 18                 |
| Table 3.2. Atomic densities of the first wall candidate materials .....  | 20                 |
| Table 3.3. Atomic densities of the candidate coolant materials.....  | 21                 |
| Table 4.1. DPA and He Structural Lifetime and He/DPA ratio with respect to<br>Different First Wall Materials and Coolants..... | 46                 |



## **SYMBOLS AND ABBREVIATIONS INDEX**

### **SYMBOLS**

- n : particle/ion density  
 $\tau$  : confinement time for reaction

### **ABBREVIATIONS**

- DPA : Displacement Per Atom  
TBR : Tritium Breeding Ratio  
ITER : International Thermonuclear Experimental Reactor  
FW : First Wall  
ENDF : Evaluated Nuclear Data File  
CLAW : Activity Cross Section Data Library  
TOKAMAK : Toroidalnaya Kamera and Magnitnaya Katushka

## **CHAPTER 1**

### **INTRODUCTION**

#### **1.1. BACKGROUND**

One of the fundamental criteria for technological development is energy consumption in the twenty-first century and as a measure of mentioned development, and energy consumption increases in direct proportion to countries' development. Humanity continues to work towards a more efficient use of existing energy resources and research for new energy resources to cope with this increasing energy consumption. The most important sources of energy under investigation are nuclear energy. Compared to renewable energy generation methods, nuclear energy delivers a much larger amount of energy at any time of year. At the same time, nuclear energy provides the consumer with the necessary energy sustainably with less fuel consumption and zero carbon emissions.

Today's nuclear power plants use fission reactions, in which the fragmentation of the atom obtains energy. The limited reserves of uranium used as fuel in fission reactors are the biggest obstacle to sustainable energy production in fission reactors. Moreover, long and short-lived radioactive wastes released during the operation of fission reactors can cause environmental disasters if they are not stored in accordance with the protocols. However, unlike fission reactors, fusion reactors can meet sustainable nuclear energy needs with almost unlimited fuel potential via the massive amount of energy released from the fusion reaction of deuterium and tritium. Today, scientists and engineers are enthusiastic about the applicability of fusion technology because of the abundance of fuels used in fusion reactions, their easy availability, and the lack of risk of reactor melting or loss of control.

It is different from the energy of other atomic phenomena such as ordinary chemical reactions, which only affect the orbital electrons of atoms, one way to release nuclear power is to control nuclear fission in devices called reactors that now operate in many parts of the world to produce electricity, another way of getting nuclear power is nuclear fusion, nuclear power has been released through nuclear fusion and nuclear fission [1].

A nuclear reactor is a device used to initiate and control a nuclear fission chain reaction or nuclear fusion reactions. Nuclear reactors are used in nuclear power plants to generate electricity and in nuclear marine propulsion. The heat from nuclear fission is passed to a working fluid (water or gas), which in turn passes through a steam turbine. These either drive the ship's propellers or drive the shafts of electric generators. Nuclear-generated steam can in principle be used for industrial process heat or district heating. Some reactors are used to produce isotopes for medical and industrial use.

There are two basic nuclear processes for energy production: fission and fusion, Fission is the active splitting of large atoms such as uranium or plutonium into two smaller atoms, called fission products. To split an atom, you have to hit it with a neutron. Many neutrons are also released that can continue to split other nearby atoms, resulting in a nuclear chain reaction to release sustained energy. This nuclear reaction was the first to be discovered. All commercial nuclear power plants in operation use this reaction to generate heat that turns into electricity. Fusion is the fusion of two small atoms such as hydrogen or helium to produce heavier atoms and energy. These reactions can release more energy than fission without producing many radioactive byproducts. Fusion reactions occur in the Sun, generally using hydrogen as fuel and producing helium as waste.

There are several sources of energy including renewable energy such as solar energy, wind energy, hydroelectric power, geothermal energy and non-renewable ones such as oil, coal, oil shale and nuclear energy. Nuclear energy considers one of the energy sources that provide sustainable and environmentally friendly power generation and provides a large amount of energy to consumers around the clock compared to renewable energy generation methods, with less fuel consumption and zero carbon

emissions, compared to energy production facilities that use fossil fuels. It is easy for humanity to completely abandon fossil energy, such as oil or coal, which emits dense carbon dioxide, and hydrogen fusion can also replace the nuclear energy produced by conventional atomic reactors, so if the fission of an atom produces radioactive waste for tens Thousands of years, hydrogen fusion would not generate long-term waste. One of the advantages of the new reactor is that the fuel needed for this fusion extracted from water and lithium salt is available. Nuclear fusion has the potential to provide sufficient energy to meet the growing demand for it around the world, while doing so sustainably, without significantly affecting the environment. Nuclear reactors use the nuclear fission process to obtain energy by splitting the nucleus of a heavy atom into two or more parts, and with this process, a certain element transforms into another element, and the fission process results in high-energy neutrons and photons (especially gamma rays) and nuclear particles such as alpha particles and beta rays. The fission of heavy elements generates huge amounts of heat and radiation energy. The high cost of uranium and plutonium used as fuel in fission reactors is the biggest obstacle to sustainable energy production in fission reactors, The long and short-lived radioactive wastes emitted during the operation of the fission reactors may cause environmental disasters if they are not storing them according to protocols because the waste in question poses a risk to the storage and the environment.

Unlike fission reactors, fusion reactors have the ability to produce sustainable nuclear energy with abundant and inexpensive fuel potential. In the 1920s, the principles of fusion reactions were investigated, and it found that fusion reactions are the source of energy produced in stars, the mathematical formulas and Robert Descarton Atkinson and Fritz Huttermann created models for fusion reactions that take place in stars in their studies. In their study, Atkinson and Hoterman showed that fusion reactions can be performed at lower temperatures than star interactions. Due to these studies carried out in the 1920s, the development of fusion reactors, which was discussed in the 1950s, accelerated. The development of fusion reactors, discovered by Stellerator, discovered by Lehman Spitzer in 1951, and by Richard F Post and Jericho Podker in the mid-1950s, through independent work, are the two most important examples. However, TOKAMAK, which was developed by Soviet research in the late 1960s, has been adopted as the most promising configuration of fusion reactors and from the 1960s to

the present, the TOKAMAK configuration has been developed and reached a position that provides energy acquisition unlike other fusion reactors. In 2010, construction of the ITER project, the world's largest fusion reactor project, began in cooperation with China, the European Union, India, Japan, Russia and the United States, with contributions from 35 countries. With this reactor, which will have commissioned in 2035, the first fusion reactor that will provide net energy gains from fusion will be completed. In this way, fusion reactors will become more important; it is expected that they would be the solution to the global energy path.

## **1.2. NUCLEAR FUSION**

Nuclear fusion is a reaction process when at least two light nuclei collide to form a heavier nucleus. Nuclear fusion occurs in low-atomic-number elements, such as hydrogen. Fusion is the opposite of nuclear fission interaction where heavy elements spread and form lighter elements. Both nuclear fusion and fission produce an enormous amount of energy. When two or more atomic nuclei merge to form a single, heavier nucleus, part of the nucleus mass transform to energy because the new core mass is less than the original mass, based on the principle of mass-energy equivalence, this mass difference means that some mass has been converted into energy, For elements lighter than iron, fusion yields energy. For elements lighter than iron, it is instead a process of fission that results in a yield of energy when deuterium and tritium merge together, their components combine to form a helium atom and rapid neutrons. When the two heavy isotopes are reintegrated into the helium and neutron atom, the additional mass of the remains turns into kinetic energy. Figure 1.1. shows a typical nuclear fusion reaction.

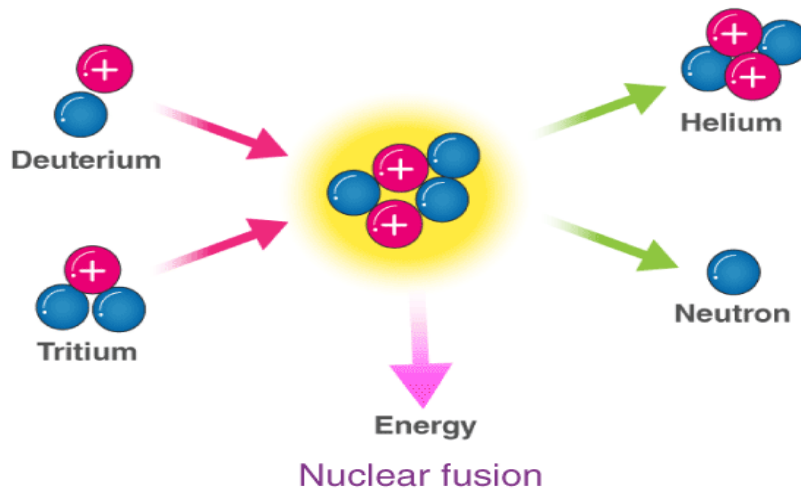


Figure 1.1. A typical nuclear fusion reaction.

The most basic fusion reactions are deuterium-deuterium (D-D) and deuterium-tritium (D-T) reactions.

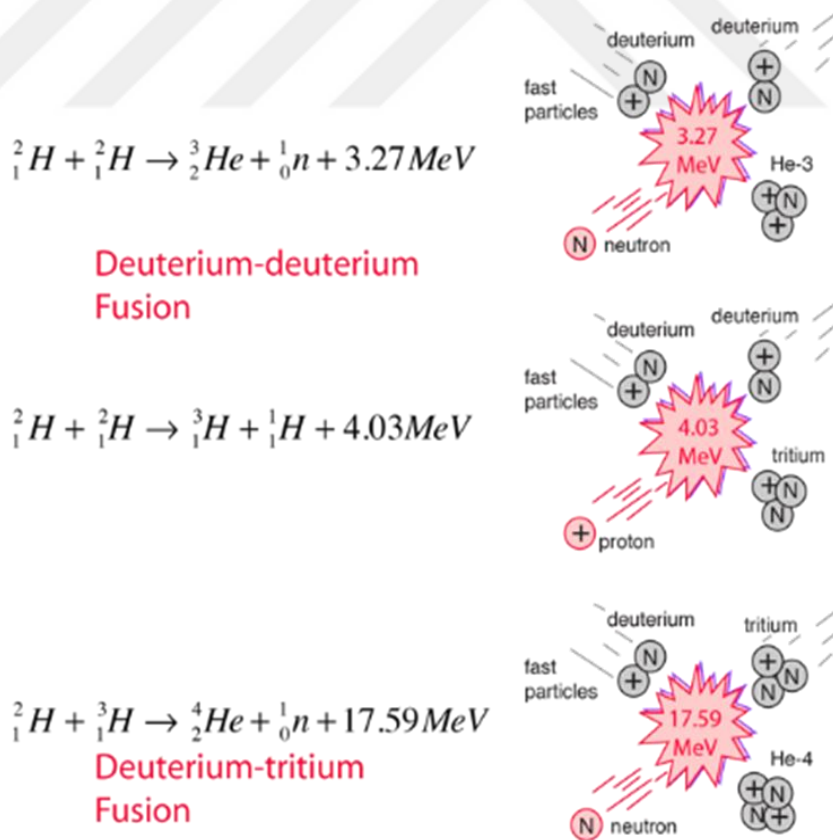


Figure 1.2. D-D and D-T nuclear fusion reaction.

Deuterium-tritium fusion is the most promising interaction for hydrogen fusion, and tritium occurs naturally only in small quantities (caused by cosmic rays) and is radioactive and has a half-life of 12 years. The most promising source of tritium appears to be the multiplication of tritium from Li-6 by slow neutron bombardment with the reaction which occurs if lithium is used as a refrigerant and the medium of heat transfer around the reaction chamber of the fusion reactor. Figure 1.2. shows a representative picture of D-D and D-T nuclear fusion reactions.

### 1.3. FUSION IN STARS

The temperature in the core of the Sun is about 15 million degrees Celsius and the gas density is about  $160 \text{ gr/cm}^3$  because of gravity coupled with very high pressure, the hydrogen and helium gas combine to become plasma and separate electrons from the nucleus to give a combination of positive charges ions and electrons.

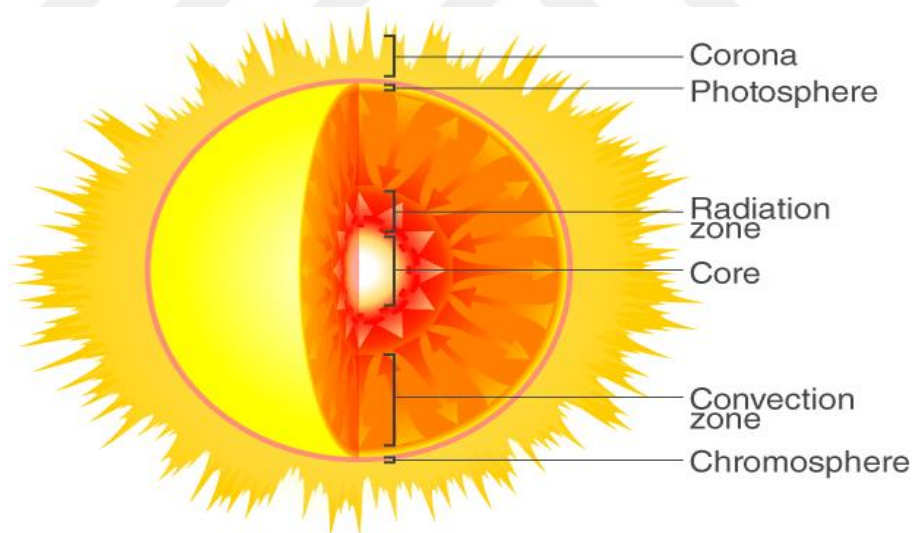


Figure 1.3. Fusion in stars [2].

Under these conditions protons (H-1) react with other protons to make deuterium nuclei (H-2) and positrons. The deuterium nuclei can merge to form a helium nucleus (He-4), or they can interact with other protons to make another isotope of helium (He-3). Two He-3 nuclei can fuse to make a nucleus of an unstable beryllium nucleus (Be-

6) that breaks apart to give He-4 and two protons. Figure 1.3. and Figure 1.4. show a fusion in stars and energy is released at each step, respectively [2].

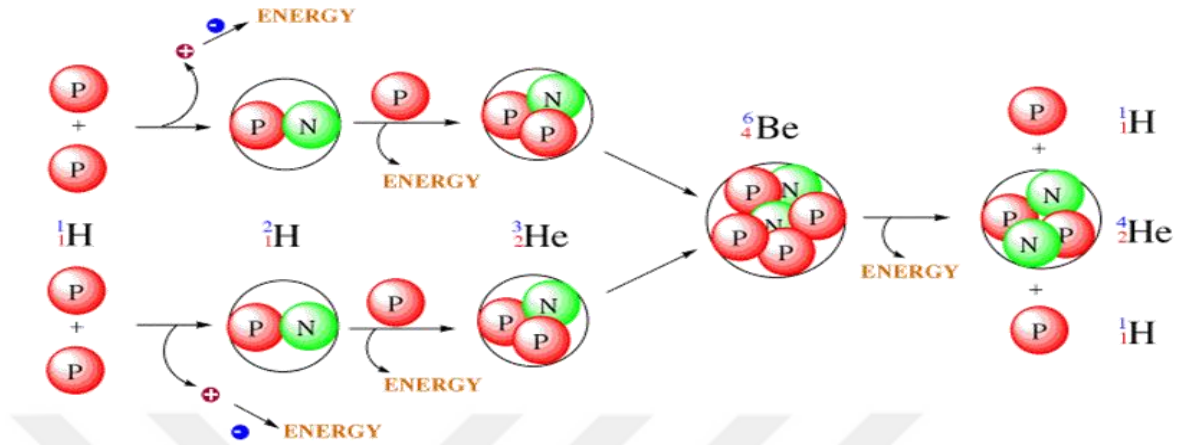


Figure 1.4. Energy released at each step.

#### 1.4. APPLICATION OF FUSION IN ENERGY PRODUCTION

At present, there are no large-scale fusion reactors capable of saving energy, this is due to the fact that it was difficult for scientists to create a manageable and non-destructive means of harnessing the energy released during the merger. The merger is difficult to control in large part because of the harsh conditions necessary for feedback to occur. The fusion requires high temperatures to give hydrogen atoms sufficient energy to overcome Coulomb's repulsion between protons, and the energy generated by microwave or laser should be used to heat hydrogen atoms at required temperatures, in addition, hydrogen atoms must be close enough together for strong nuclear power to start working, high pressures are needed to squeeze hydrogen atoms and make them close enough to merge again using intense magnetic fields, lasers or ion rays [1].

##### 1.4.1. Conditions For Fusion

The fusion reaction requires providing a high enough temperature to enable particles to overcome the Coulomb barrier, the temperature must be maintained long enough and with sufficient ion density in order to sustain the reaction and obtain sufficient energy from the fusion reaction. The overall requirements for producing more energy than

required for plasma heating are determined in terms of the ion density product and confinement time, a condition called the Lawson Standard [3]. Lawson's criterion for fusion:

$$n\tau \geq 10^{14} \text{ S/cm}^3 \text{ deuterium - tritium fusion}$$

$$n\tau \geq 10^{16} \text{ S/cm}^3 \text{ deuterium - deuterium fusion}$$

### 1.4.2. Confinement Time

Confinement time in nuclear fusion devices is defined as the time during which the plasma is kept at a temperature higher than the critical ignition temperature, to produce more energy from fusion than has been invested to heat the plasma, the plasma must be held at this temperature for a minimum of time [3].

$$\text{Deuterium- Tritium fusion} \quad \tau = \frac{2 \times 10^{14}}{n} \text{ S}$$

$$\text{Deuterium- Deuterium fusion} \quad \tau = \frac{5 \times 10^{15}}{n} \text{ S}$$

### 1.4.3. Ion Density

Although there is a high enough temperature to overcome Colum's barrier to nuclear fusion ion density must be maintained to make the probability of binding high enough to achieve a net energy yield from the reaction and the intensity required to produce energy is associated with the time of accounting for hot plasma, Therefore, the minimum requirement of the normally produced fusion reaction is determined in terms of the ion density output and confinement time.

$$\text{Deuterium - tritium fusion} \quad : n\tau = 2 \times 10^{14} \text{ s/cm}^3$$

$$\text{Deuterium - deuterium fusion:} \quad : n\tau = 5 \times 10^{15} \text{ s/cm}^3$$

#### 1.4.4. Fusion Reactors

There are two main types of fusion reactors: magnetic confinement reactors and inertial confinement reactors, The Strategies for creating fusion reactors are largely dictated by the fact that the temperatures involved in nuclear fusion are very high so that they cannot be contained in any material container. The work of the inertial confinement reactor is to place this high energy density in the small pellets of deuterium and tritium that merge in such a short time that they cannot move significantly, more advanced test reactors include laser fusion. The magnetic confinement reactor strategy is to confine hot plasma through the magnetic fields that keep it permanently in the paths of the rings that do not touch the container wall. This was categorized by TOKAMAK Design seen in Figure 1.5. [1].

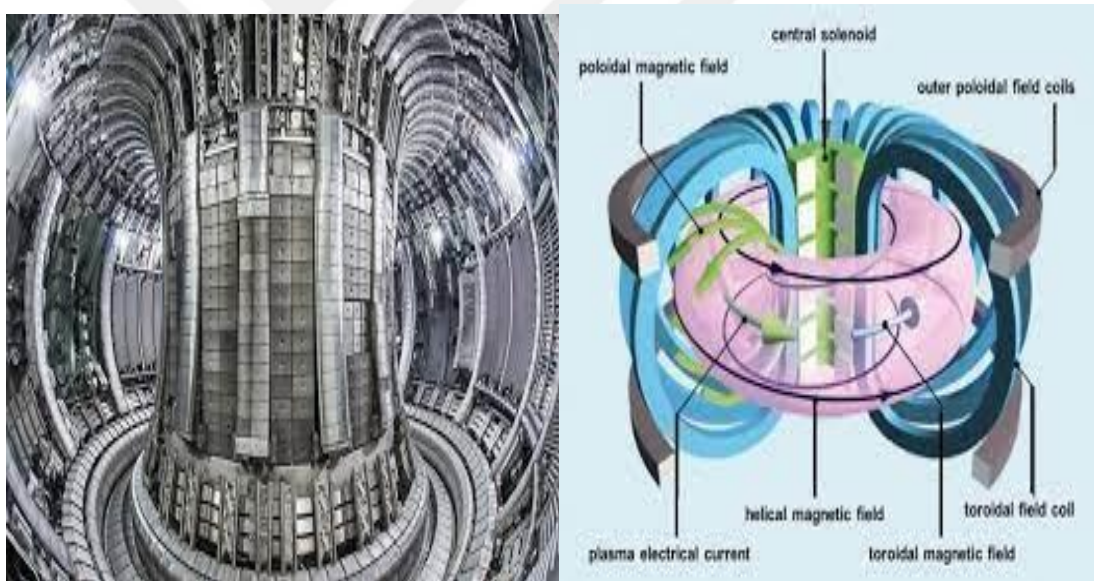


Figure 1.5. Magnetic confinement reactor (TOKAMAK) [1].

#### 1.5. AIMS AND OBJECTIVES

The aim of the thesis is to study the effects of changing the first wall material and its thickness on the reactor and displacement per atom (DPA) and the gas production (He and H) in the first wall and the tritium reproduction ratio (TBR) in the cooling area and tritium breeding area. Magnetic fusion reactor modelling will be determined based on ITER's overall parameters. Stainless steel (SS 316 LN-IG), reinforced steel alloy

for oxide dispersion (PM2000 ODS) and Chinese low activation martensitic steel (CLAM) will be used as first wall material (FW). Molten salt materials from the fluoride family (FLiBe, FLiNaBe, FLiPb) and lithium oxide (LiO<sub>2</sub>) will be cooled and tritium production material in the blanket, respectively. Neutron transport calculations will be made by the well-known 3D code MCNP5 using Monte Carlo's continuous energy methods. Using the latest built-in continuous nuclear and atomic power libraries, the evaluated nuclear data file system (ENDF/B-V and ENDDF/B-VI), the FORTRAN 90 interface computer software will be used to assess the MCNP5 outputs of the fusion reactor blanket.



## CHAPTER 2

### LITERATURE OVERVIEW

Research on fusion energy for electricity production has primarily focused on the concepts of magnetic and inertial fusion energy. In the last 70 years, the concept of magnetic fusion has gained importance in the field of electricity generation from fusion energy. El-Guebaly [4] stated that the magnetic fusion concept based on a toroidal configuration of Toroidalnaya Kamera and Magnitnaya Katushka/Toroidal Chamber and Magnetic Coil (TOKAMAK) devices, and the International Thermonuclear Experimental Reactor (ITER) is one of the most important pioneers of this concept [5].

Several vital elements makeup the successful design of magnetic fusion reactors. The first element is the self-sufficient fuel cycle for plant sustainability. To design a self-sustained D-T fueled fusion reactor, tritium must be produced at least as much as it is consumed [6]. The ratio of tritium production to its consumption is determined as the net tritium breeding ratio (TBR), and to ensure its self-sufficiency, the TBR must be greater than 1.05 ( $TBR > 1.05$ ) [7]. This is because a fraction of the fuel is commonly burned up in plasma, radioactive decay of tritium, and calculation uncertainties [8]. Studies in literature show that different concepts examine the TBR in fusion reactors. Hernández and Pereslavitsev [9] investigated the solid tritium breeder concept for use in fusion reactors. The TBR of all solid tritium breeders were sufficient for operating the reactor sustainably, and  $Li_3N$  showed the highest tritium breeding performance. The tritium breeding performance of a solid breeder blanket for (demonstration power station) was examined, and they found that  $Li_4SiO_4$  had the best tritium breeding performance [10].

According to varying cooler thicknesses, neutronic analysis of a magnetic fusion reactor with spherical geometry was performed using FLiBe ( $Li_2BeF_4$ ) as a coolant [11]. According to the findings, the TBR value was sufficient for sustainably operating

the reactor, and the optimum coolant thickness was 50 cm. In the 1960s, FLiBe was used as the molten salt (MS) in molten salt reactor experiments (MSRE). The neutronic performance of liquid metals and molten salts in the blanket of a hybrid reactor has been examined [12,13]. It was observed that a model in which natural lithium was used as a coolant exhibited the highest TBR performance. The tritium breeding potential of Li-Sn has been investigated, and it has been determined that when the thick-liquid-breeder concept is applied, the tritium breeding potential of Li-Sn better is than FLiBe [14]. Youssef compared the tritium breeding potential of FLiBe and FLiNaBe, which have favorable melting points, and observed that the tritium production potential of FLiBe was higher than FLiNaBe [15].

The tritium breeding ratio of the fusion-fission hybrid reactors with different molten salts was investigated [16] and the findings of this study determined that the highest TBR value was obtained when 90 % enriched lithium was used as a coolant in the model. Despite the high TBR values obtained in studies using natural or enriched lithium, the radiation damage and energy multiplication factors of the blanket structure of the reactor should be carefully examined. On this basis, FLiBe is a much more appropriate coolant than natural lithium, as it has both a sufficient TBR and causes a higher energy multiplication factor and low radiation damage. The effects of varying the lithium enrichment rates and SS304 material used in the first wall on the neutronic performance of the hybrid reactor were examined [17]. The calculations show that the lithium enrichment rate is directly proportional to the total TBR and inversely proportional to the displacement per atom (DPA). The vanadium alloy provided the best results in terms of the TBR value, and the copper alloy gave the best result in terms of DPA. In this study, the effect of changing the coolers and first wall materials on the neutronic performance of hybrid reactors was examined [18]. The best coolant performance was obtained when FLiBe was used; W-5Re, TZM, T111, and Nb-1Zr were used as the first wall materials. The calculations showed that the worst tritium production performance was obtained when the T111 material was used, whereas the tritium production performance of the other materials was found to be very close to each other. SS304, SS316, ODS, Mo, vanadium, and W were used as the first wall materials in the blanket structure fusion, whereby hybrid reactors were investigated [19]. The highest TBR and lowest radiation damage were observed for vanadium and

W, respectively. In addition to liquid metals and molten salt coolants in magnetic fusion reactors, gas coolants can be used to make necessary design changes. The effect of the He/LiPb coolants on the neutronic performance of the reactor was examined [20]. Despite sufficient tritium production, the coolant zone of the reactor must be designed for operation at high pressures and temperatures. Wang et al. [21] analyzed the efficiency of CO<sub>2</sub>-and He-cooled DEMO fusion power plants and found that helium (He) performed better in terms of gross and net efficiencies. Tillack et al [22] summarized existing design concepts and parameters for fusion power plants using He as the coolant material and determined that the heat removal capability of He is not worse than that of water in a well-designed system but noted that an increase in pump power is necessary to work with high pressure values.

According to the findings obtained from previous studies, the lithium concentration in the coolant materials directly affects tritium production, and neutron breeder isotopes provide a sufficient tritium breeding ratio for autonomous fusion reactor operation. Romatoski and Hu [23] recommended experimental and theoretical property data for candidate fluoride salt coolants for use in nuclear applications. They investigated neutronic and coolant thermophysical properties, such as density, heat capacity, thermal conductivity, and viscosity [23]. In addition, the properties (melting points, densities, neutron multiplier, TBR) of the molten salt materials (FLiBe, FLiNaBe, FLiPb), belonging to the family of fluorides with their references in the literature, have been reported [24].

The second element for a successful fusion reactor design is to protect the reactor structure from high-energy neutrons released from the plasma. As such, a layer should be placed between the plasma and reactor layers. The mentioned layer is known as the first wall and can be designed using two essential concepts: solid and liquid. Nevertheless, the solid wall concept is preferred owing to the high neutron damage and wall load in fusion reactors, the liquid wall concept is preferred for hybrid reactors with low wall loads [25, 26].

Tunç et al. [27] investigated the radiation damage parameters of oxide dispersion strengthened (ODS) steel alloys. According to the results of tritium production, gas

production, and nuclear heating calculations, the 12YWT steel showed the best performance. A comprehensive study on the neutronic performance of reduced activation ferritic/martensitic steels (RAFM) (such as EUROFER97 and F82H), vanadium alloys, silicon carbide, copper alloys, and stainless steel (SS 316) as the first wall materials has been conducted. V4Cr4Ti and Cu0.5Cr0.3Zr exhibited the best tritium breeding, gas production, and DPA performance in this work [7]. In addition to ODS steels, vanadium and copper alloys can also be used as the first wall material in fusion reactors. Muroga [28] used vanadium alloy as the first wall material and FLiBe as the coolant. According to the study results, the reactor produced self-sufficient tritium and the superconductor magnet systems were protected from neutron damage. The Institute of Plasma Physics, Chinese Academy of Sciences (ASIPP), has conducted a series of research and development studies on CLAM as a structural material and related technology. A summary of these studies was presented by Huang et al., primarily covering the composition design, property tests, techniques for joining and coating, and activation analysis, which are corrosion properties of liquid LiPb and irradiation effects from plasma. These studies show that CLAM has some good properties before irradiation from the current test. Huang et al. [29] provided the chemical composition of CLAM, which is based on extensive research from various ongoing international research and development programs on RAFMs.

In contrast to other studies in literature on the neutronic performance of fusion reactors, this study aimed to determine the effect of the material composition and thickness of the first wall on the reactor's neutronic performance, such as tritium breeding materials and first wall material damage. Modeling of a magnetic fusion reactor was completed based on ITER's blanket parameters of the ITER. Stainless steel (SS 316 LN-IG), steel alloy (PM2000 ODS), and CLAM were used as FW materials. The effects of changing the first wall materials and their thickness on the reactor were investigated in the DPA and gas production in the first wall, as well as the TBR in the coolant zone and tritium breeding zone. Therefore, in the blanket, fluoride family molten salt materials (FLiBe, FLiNaBe, and FLiPb) as well as the neutron multiplier (Be and Pb) were used as coolants. Lithium oxide ( $\text{LiO}_2$ ) was considered as a tritium production material for comparison.

## CHAPTER 3

### METHOD

#### 3.1. DESCRIPTION OF GEOMETRICAL MODEL FOR NEUTRONIC CALCULATIONS

Figure 3.1. shows the MCNP5 geometry output of the simplified model for the neutronic analysis of the blanket structure of a magnetic fusion reactor. In this model, the reactor consists of nine layers [30].

Plasma region inside a D shaped blanket structure: In the study, deuterium-tritium fusion fuel was used in the magnetic fusion reactor due to its high energy potential. In the model where the plasma is homogeneously distributed, the minor radius of the plasma region is 200 cm and the major radius is 620 cm, and it is added to the model as a reactor component in a way that preserves the low aspect ratio.

First wall zone: In this study, the solid first wall concept was applied. Different materials (Stainless Steel (SS 316 LN-IG), Oxide Dispersion Strengthened Steel Alloy (PM2000 ODS) and China low activation martensitic steel (CLAM)) were determined as the first wall material. The effects of the thickness of the first wall (1 to 5 cm) on the neutronic performance of the reactor were investigated.

Coolant zone: In the reactor blanket, fluorides family molten salt materials, as well as the neutron multiplier and high tritium breeding performance (FLIBE, FLINABE and FLIPB), were used as a coolant. The thickness of this layer has been chosen as 50 cm in order to achieve optimum neutronic performance.

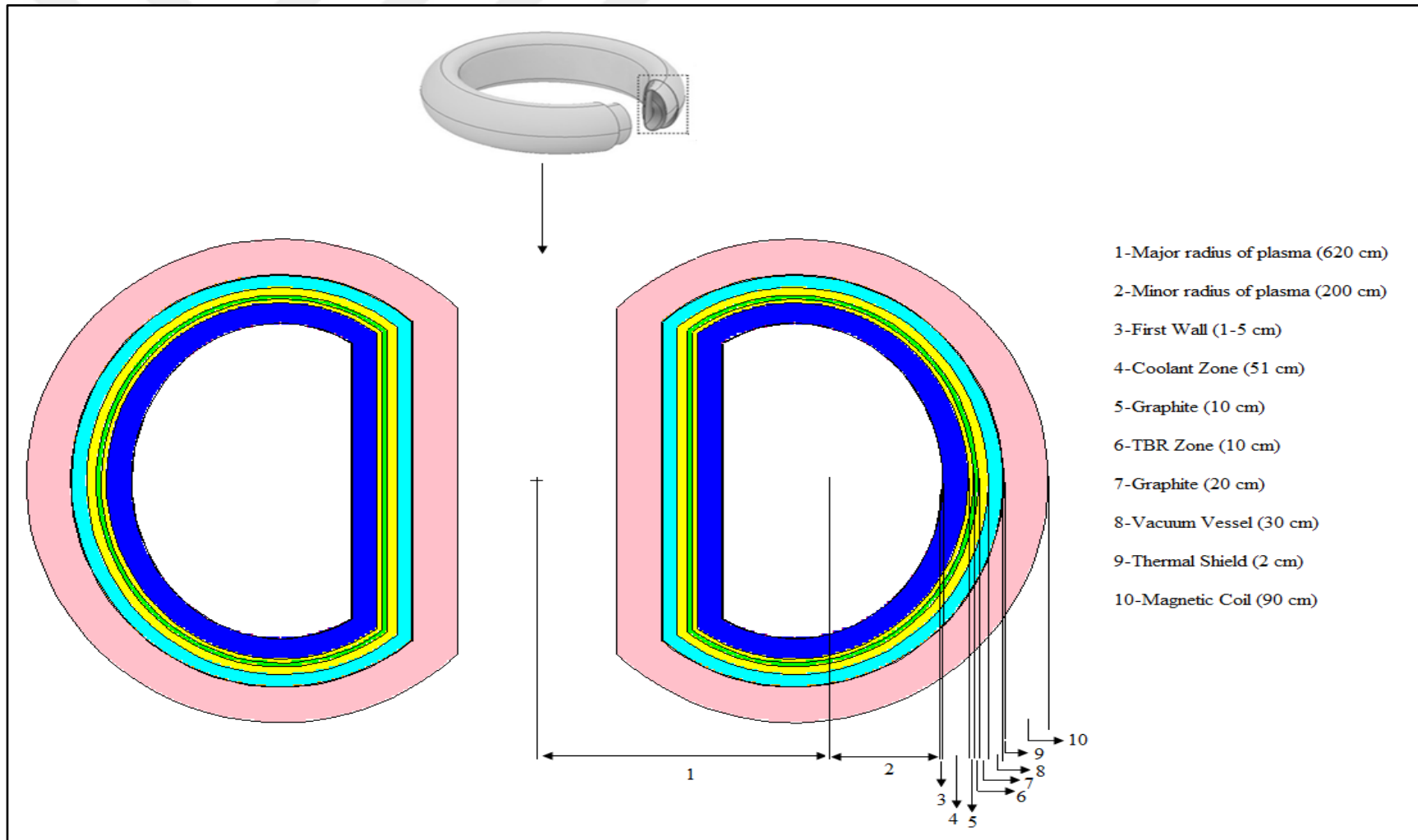


Figure 3.1. Blanket structure of investigated magnetic fusion reactor [31].

Reflector zones: First reflector zone (graphite 10 cm) was added to the reactor model after the coolant zone to reflect the neutrons from the fusion source and send them back to the coolant zone. Graphite, a material that does not react with neutrons, was used as a reflector. The second reflector zone (graphite 20 cm) was also added after the tritium breeding zone to reflect the neutrons and send them back to the tritium breeding zone. In this way, neutron damage in the reactor's magnet layer has been reduced, and an increase in tritium production and energy multiplication factor values will be observed.

Tritium breeding zone: In this layer, Lithium oxide ( $\text{LiO}_2$ ) was chosen as the tritium production material. The layer thickness was determined as 10 cm, and the tritium production potential was increased by adding a reflector zone after this zone.

Vacuum vessel: It is a safety containment barrier and supports the stability of the plasma. It provides to high vacuum environment and electrical resistivity. It has a double structure to continuity of electrical and structural continuity [32]. In this study, we assumed vacuum vessel composed of homogeneous mixture of 60 % borated steel (S30467) and 40 % water [33]. The thickness of the vacuum vessel was chosen 30 cm.

Thermal shield: When the plasma releases the heat, conductive heat transfer occurs between the blanket components. The thermal shield hampers the heat loads to reach the toroidal field coils. It is composed of stainless-steel panels and panels cooled by helium gas [5]. The material SS316LN-IG material was selected for the thermal shielding and the thickness of the shield was determined as 2 cm.

Magnetic Coil: Plasma limitation in magnetic fusion reactors is done with the help of magnets. The magnets and the plasma surrounding the reactor's outermost layer limit the plasma with magnetic force according to the limits of the designed reactor. Another function of magnets is to keep the plasma in the center of the reactor with magnetic force and prevent it from dispersing. It is assumed that magnetic coil is composed of a homogenous mixture of 45 %  $\text{Nb}_3\text{Sn}$ , 50 % Incoloy 908 and 5 %  $\text{Al}_2\text{O}_3$  [33].

Table 3.1. lists the atomic densities of the blanket materials in the different zone used in this study. Furthermore, Table 3.2. shows the isotopic compositions and atomic densities of the candidate materials for the investigated first wall. Moreover, Atomic densities of the candidate coolant molten salt materials are given in Table 3.3.

Table 3.1. Atomic densities of the blanket materials [31].

| Blanket Zone | Material                      | Specific Weight (gr/cm <sup>3</sup> ) | Nuclide  | Nuclei Density (atom/barn.cm)   |
|--------------|-------------------------------|---------------------------------------|--|---|
| 2            | First Wall Candidate          | Seen in Table 2.                      |  |   |
| 3            | Coolants                      | Seen in Table 3.                      |  |   |
| 4            | Reflector (Graphite)          | 2.267                                 | C-12   | 1.13661E-01   |
| 5            | TBR Zone (Lithium oxide)      | 2.013                                 | Li-6<br>Li-7<br>O-16                           | 6.15851E-03<br>7.49813E-02<br>4.05699E-02   |
| 6            | Reflector (Graphite)          | 2.267                                 | C-12   | 1.13661E-01   |
| 7            | Vacuum vessel S30467 (60 %)   | 7.8                                   | Fe<br>C<br>Mn<br>Cr<br>B<br>Si<br>Ni<br>H<br>O | 5.24159E-02<br>7.82143E-05<br>1.39364E-03<br>1.74350E-02<br>9.12492E-03<br>8.86414E-04<br>1.12828E-02<br>6.68566E-02<br>3.34283E-02 |
|              | H <sub>2</sub> O (40 %)       | 1                                     |  |   |
| 8            | Thermal Shield (SS 316 LN-IG) | 8                                     | Fe<br>C<br>Mn                                  | 5.65101E-02<br>4.01099E-05<br>1.57845E-03   |

Table 3.1. (continues).

|    |                                     |       |    |             |
|----|-------------------------------------|-------|----|-------------|
|    |                                     |       | P  | 3.11074E-05 |
|    |                                     |       | S  | 1.50268E-06 |
|    |                                     |       | Si | 6.86146E-04 |
|    |                                     |       | Ni | 1.00948E-02 |
|    |                                     |       | Cr | 1.61217E-02 |
|    |                                     |       | Mo | 1.20515E-03 |
|    |                                     |       | N  | 2.06424E-04 |
|    |                                     |       | Nb | 1.03709E-05 |
|    |                                     |       | Cu | 2.27438E-05 |
|    |                                     |       | Co | 2.45240E-05 |
|    |                                     |       | B  | 4.01095E-06 |
|    |                                     |       | Ta | 2.66242E-06 |
|    |                                     |       | Ti | 1.00576E-05 |
| 9  | Coil<br>Nb <sub>3</sub> Sn (45%)    | 8.4   | Nb | 1.71828E-02 |
|    |                                     |       | Sn | 5.72759E-03 |
|    |                                     |       | Al | 2.35482E-03 |
|    | Al <sub>2</sub> O <sub>3</sub> (5%) | 3.987 | O  | 3.53223E-03 |
|    |                                     |       | Fe | 1.79278E-02 |
|    |                                     |       | Ni | 2.05348E-02 |
|    | Incoloy 908<br>(50%)                | 8.17  | Cr | 1.88298E-03 |
|    |                                     |       | Nb | 7.73161E-04 |
|    |                                     |       | Ti | 8.93607E-04 |
|    |                                     |       | Al | 8.47909E-04 |
|    |                                     |       | N  | 3.51351E-06 |
|    |                                     |       | Mn | 1.83588E-05 |
|    |                                     |       | C  | 2.04811E-05 |
| Co | 4.17419E-05                         |       |    |             |

Table 3.2. Atomic densities of the first wall candidate materials [31].

| Nuclide | Nuclei Density (atom/barn.cm)   |                           |  |
|---------|---------------------------------|---------------------------|--|
|         | SS 316 LN-IG<br>Stainless Steel | PM2000<br>ODS Steel Alloy | CLAM (China low activation<br>martensitic steel) |
| Al      | -                               | 8.22968E-03               | -  |
| B       | 4.01095E-06                     | 1.20830E-06               | -  |
| C       | 4.01099E-05                     | 3.62493E-05               | 3.90069E-04                                      |
| Co      | 2.45240E-05                     | 7.38789E-06               | -  |
| Cr      | 1.61217E-02                     | 1.58427E-02               | 8.10948E-03                                      |
| Cu      | 2.27438E-05                     | 6.85158E-06               | -  |
| Fe      | 5.65101E-02                     | 5.82026E-02               | 7.42966E-02                                      |
| Mn      | 1.57845E-03                     | 8.71764E-05               | 3.83760E-04                                      |
| Mo      | 1.20515E-03                     | 4.53768E-06               | -  |
| N       | 2.06424E-04                     | 8.70346E-06               | 6.69159E-05                                      |
| Nb      | 1.03708E-05                     | -                         | -  |
| Ni      | 1.00948E-02                     | 7.41810E-06               | -  |
| O       | -                               | 6.80340E-04               | -  |
| P       | 3.11074E-05                     | 2.81133E-06               | 4.53779E-06                                      |
| S       | 1.50268E-06                     | 2.85190E-06               | 2.92272E-06                                      |
| Si      | 6.86146E-04                     | 6.20104E-05               | 1.66819E-05                                      |
| Ta      | 2.66242E-06                     | -                         | 3.88381E-05                                      |
| Ti      | 1.00576E-05                     | 4.09313E-04               | 5.86275E-06                                      |
| V       | -                               | -                         | 1.83939E-04                                      |
| W       | -                               | 9.47325E-06               | 3.82271E-04                                      |
| Y       | -                               | 1.81196E-04               | -  |
| Zr      | -                               | 4.77276E-06               | -  |
| Total   | 8.65498E-02                     | 8.37873E-02               | 8.38818E-02                                      |

Table 3.3. Atomic densities of the candidate coolant materials [31].

| Nuclide | Nuclei Density (atom/barn.cm)           |   |  |
|---------|---|---|--|
|         | FLiBe                                   | FLiPb                                   | FLiNaBe  |
|         | LiF (67 %) +<br>BeF <sub>2</sub> (33 %) | LiF (40 %) +<br>PbF <sub>2</sub> (60 %) | LiF (35 %)-NaF (27 %)-BeF <sub>2</sub><br>(38 %) |
| Density | 1.94                                    | 3.545                                   | 2.0  |
| Li-6    | 1.80234E-03                             | 4.11519E-04                             | 8.35829E-04                                      |
| Li-7    | 2.19439E-02                             | 5.01034E-03                             | 1.01764E-02                                      |
| Be-9    | 1.16959E-02                             | -                                       | 1.19562E-02                                      |
| F-19    | 4.71381E-02                             | 2.16875E-02                             | 4.34197E-02                                      |
| Na-23   | -                                       | -                                       | 8.49516E-03                                      |
| Pb-206  | -                                       | 2.07386E-03                             | -  |
| Pb-207  | -                                       | 1.79735E-03                             | -  |
| Pb-208  | -                                       | 4.26158E-03                             | -  |
| Total   | 8.25802E-02                             | 3.52421E-02                             | 7.48833E-02                                      |

### 3.2. NEUTRON TRANSPORT EQUATION

Possible solutions methods are used, these are:

1. Analytical methods. They provide a full solution to the transport equation very limited.
2. Deterministic methods. They approximate the parameter space (e.g., discrete cross-sections) results in a full solution
3. Monte Carlo method. They solve a transport problem by simulating particle histories gives a local solution to the transport equation.

#### 3.2.1. Particle Transport Equation

The time dependent transport of neutral particles through a vacuum or medium.

$$\begin{aligned} & \frac{1}{v} \frac{\delta \psi(r, \Omega, E, t)}{\delta t} + \Omega \cdot \nabla \psi(r, \Omega, E, t) + \sigma(r, E) \psi(r, \Omega, E, t) \\ = & Q(r, E, t) + \int_0^\infty dE' \times \int_{4\pi} \sigma_s(r, \Omega' \rightarrow \Omega, E' \rightarrow E, t) \times \psi(r, \Omega', E', t) d\Omega' \end{aligned} \quad (3.1)$$

Boltzman equation 3.1. describes 7-dimensional phase space: 3 space, 2 direction, energy, and time. Here are:  $r$  is the position vector of a particle moving along the direction given by the unit direction vector  $\Omega$  with energy,  $E$ , at time  $t$ .

$$\sigma_s(r, E' \rightarrow E, \Omega' \rightarrow \Omega) dE. d\Omega$$

The probability per unit path length that a particle at position  $r$  with energy  $E'$  and travelling in direction  $\Omega'$  will scatter into an energy interval  $dE$  about  $E$  and into a solid angle  $d\Omega$  about  $\Omega$

$$\psi(r, \Omega, E, t)$$

The total number of particles per unit volume about  $r$  per unit energy about  $E$  and per unit solid angle about  $\Omega$  at time  $t$  and speed  $v$ .

### 3.2.2. MCNP and Interface Code Structure

The MCNP code runs with the input file that the user creates. Input file consists of information such as the problem geometry, identification of the materials used in the problem, nuclear data library containing the cross-sectional information of the selected materials, defining the location and characteristics of the neutron/photon or electron source, the type of detector to record the requested data. Input file consists of three main cards, these are cell card, surface card, and data card.

### 3.3. CALCULATION TOOLS

Neutron particle transport calculations were performed using the continuous energy Monte Carlo method with the well-known 3D code MCNP5 [34]. MCNP5 allows for a unique geometric definition limited only by the available computing power band,

which uses the built-in continuous energy nuclear and atomic data libraries such as the Evaluated Nuclear Data File (ENDF) system [35]. ENDF/B-V and ENDF/B-VI are nuclear data files evaluated in a US study coordinated by the National Nuclear Data Center at Brookhaven National Laboratory [36]. ENDF/B-V [37] and ENDF/B-VI [38] are neutron energy regimes are  $10^{-11}$  MeV to 20 MeV for all isotopes, and 150 MeV for some isotopes. In addition, the activity cross-section data library CLAW-IV [39] was used for atomic displacement cross-sections of FW structural materials to evaluate both the DPA values and gas production. An interface computer program written in the FORTRAN 90 language to evaluate the MCNP5 outputs was developed for the fusion reactor blanket. Figure 3. 2. shows the flow chart of the interface code for the assessment of the MCNP5 output, entitled MCNPAS (MCNP Assessment Code) [40]. In the first step, with the stochastic MCNP5/MCNPAS code, the MCNP5 code calculates the neutron fluxes and reaction rates in the cells and surfaces [41]. In the second step, the interface code reads the required data from the output and activity cross-section data library, CLAW-IV. Thereafter, the interface code calculates neutronic performance parameters such as TBR, DPA, gas production, and nuclear heating.

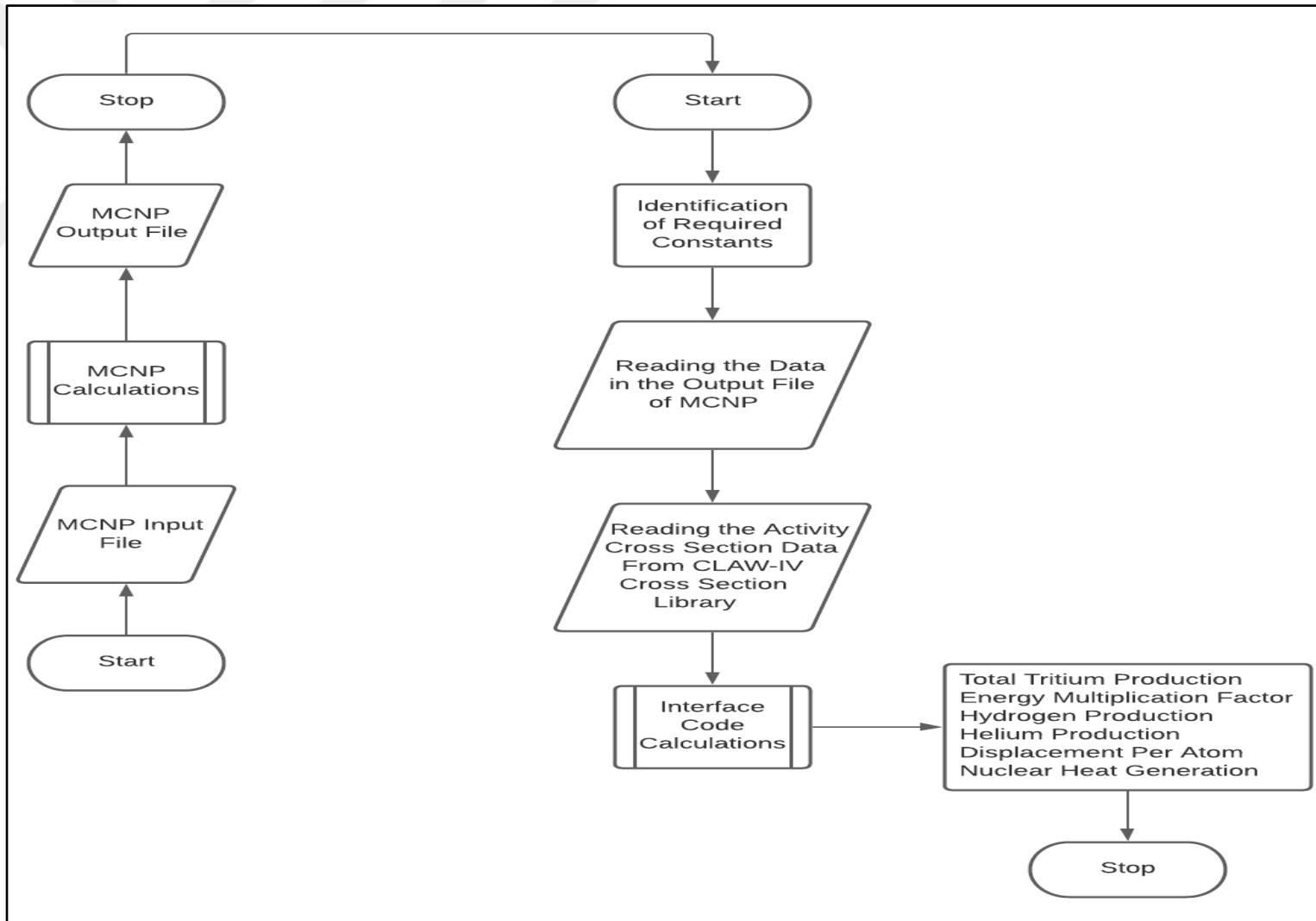


Figure 3.2. Flowchart of the problem solution [31].

## CHAPTER 4

### RESULTS AND DISCUSSION

#### 4.1. FUSION BLANKET PERFORMANCE

Fluorides family molten salt materials (FLiBe, FLiNaBe, FLiPb) as well as the neutron multiplier and Lithium oxide (LiO<sub>2</sub>) were considered as a coolant and the tritium production material in the blanket, respectively. Calculations were performed to make comparison for the fusion blanket performance.

##### 4.1.1. Tritium Breeding Ratio

Tritium is a precious and hazardous material. Since tritium is difficult to obtain and degrades with a half-life of 12.3 years, it must be produced as much as needed to be consumed. Therefore, for every triton consumed in a D-T fusion reaction, one triton must be bred in the blanket. Thus, the fusion blanket must contain a tritium-breeding material. Tritium can be produced through contact with lithium during the fusion reaction. Neutrons escaping the plasma must interact with lithium contained in the blanket to produce the tritium. Therefore, the only viable choice is lithium, which is naturally composed of 92.41% <sup>7</sup>Li and 7.59% <sup>6</sup>Li. Both isotopes breed tritium, but <sup>6</sup>Li breeds much more than <sup>7</sup>Li. In the other words, the tritium reaction cross-section increases with the decreasing neutron energy namely thermal neutrons, while cross-sections of (<sup>7</sup>Li, n) are much lower. Neutrons produce tritium in the following reactions for both isotopes in Equation 4.1 and Equation 4.2.



As can be seen from the reactions, one neutron produces only one tritium atom in the ( ${}^6\text{Li}, n$ ) reaction. In addition, Equation 4.1, the exoenergetic neutron absorption in  ${}^6\text{Li}$  occur the tritium breeding and the important effect of heat generation. A neutron multiplier is to be added to increase the efficiency of tritium breeding. Beryllium (Be) is mainly neutron multiplier, Lead (Pb) is also considered in some concepts of tritium breeding blankets [42].

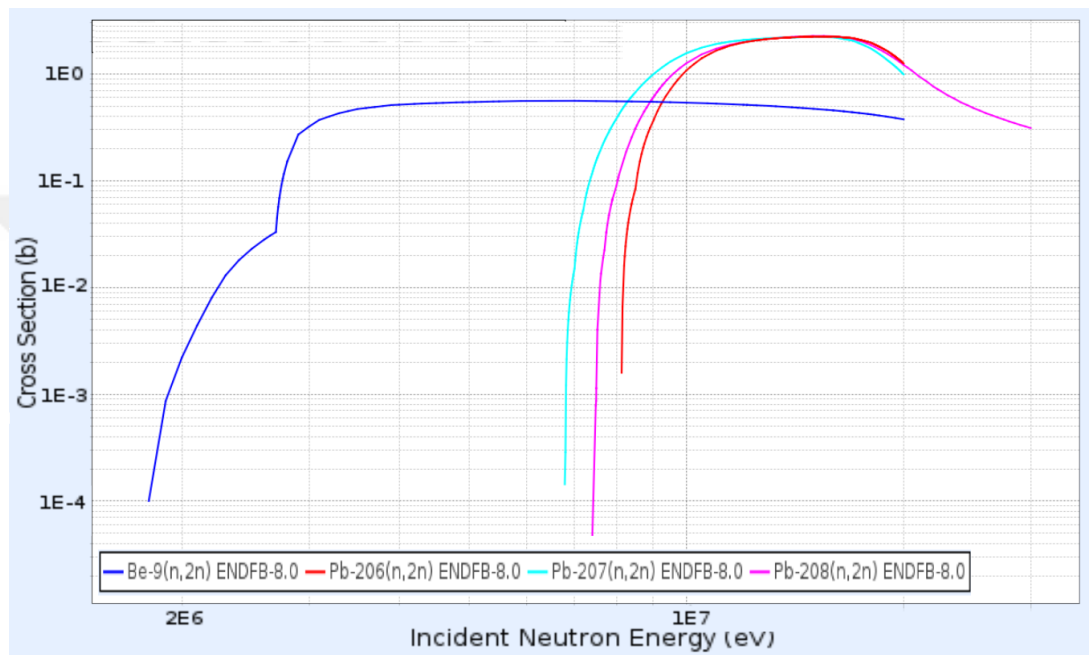


Figure 4.1. Cross Section of Be(n,2n) and Pb(n,2n) at the KAERI Nuclear Data Center.

As can be seen in the Figure 4.1., high energy neutrons (14 MeV) have a higher cross-section of Pb(n,2n), whereas thermal neutrons have a higher cross-section of Be(n,2n) [43]. In addition, as shown in Figure 4.2., the coolant zone exhibits a high-energy neutron spectrum. Therefore, the lead-containing coolant increases higher efficiency tritium breeding. For this reason, Tritium Breeding Ratio (TBR) production was investigated in two regions of the blanket layers. These effects are also clearly seen in Figure 4.3., Figure 4.4 and Figure 4.5., when comparing the TBR performance of coolants for SS 316 LN-IG, PM2000 ODS and CLAM steel alloy first wall material, respectively. TBR production rates in these two regions are given separately in Figure 4.3., Figure 4.4 and Figure 4.5. These are the coolant zone and the tritium breeding zone. If the Figure 4.3., Figure 4.4 and Figure 4.5. are examined, the contribution of

the lead-containing (Pb) coolant (FLiPb) to total TBR, is clearly observed that there is a sharp increase the tritium production in the Tritium Breeding Zone namely LiO<sub>2</sub> zone. Among the three different First Wall materials, the best performance of total TBR value is for the FLiPb coolant. Moreover, when the first wall is 2 cm for all materials, the TBR value produced in the coolant zone is sufficient.

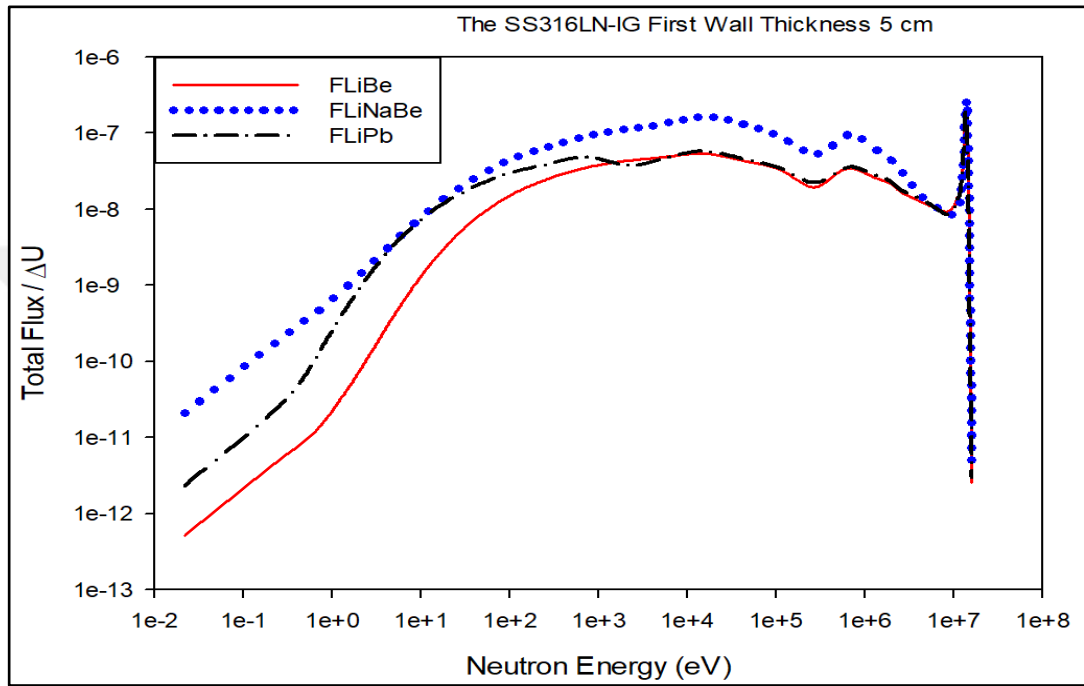


Figure 4.2. The coolants neutron spectrum at coolant region (with 5 cm SS316LN-IG First wall Thickness)

In addition, the first wall which is the first layer of the blanket on the plasma side must be made of steels with strong structure to resist fusion plasma damage and protect the blanket. It affects the reaching of high-density metal fusion neutrons to the TBR region and the amount of TBR production. In order to measure the effect of first wall thickness, the TBR is calculated for various materials used in the first wall. Because more neutrons are moderated after travelling through the thick first wall, to observe this effect, 3 different materials were used as the first wall material by changing from 1 cm to 5 cm.

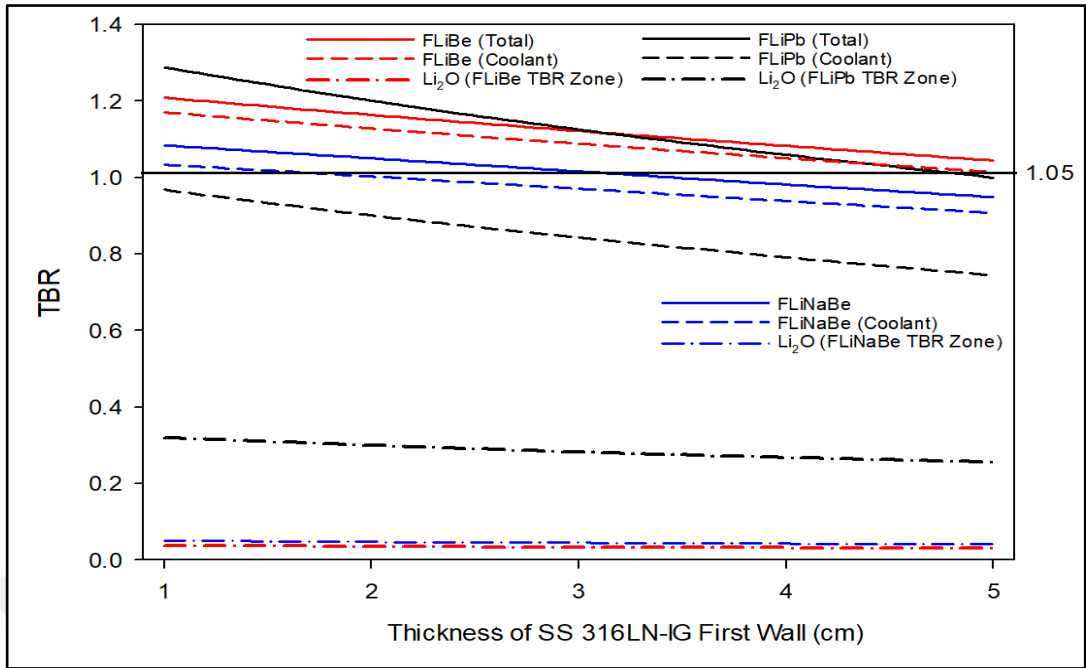


Figure 4.3. The Change of Tritium Breeding Ratio with respect to Thickness for SS 316 LN-IG Steel Alloy First Wall Material (given separately in the coolant zone and the tritium breeding zone).

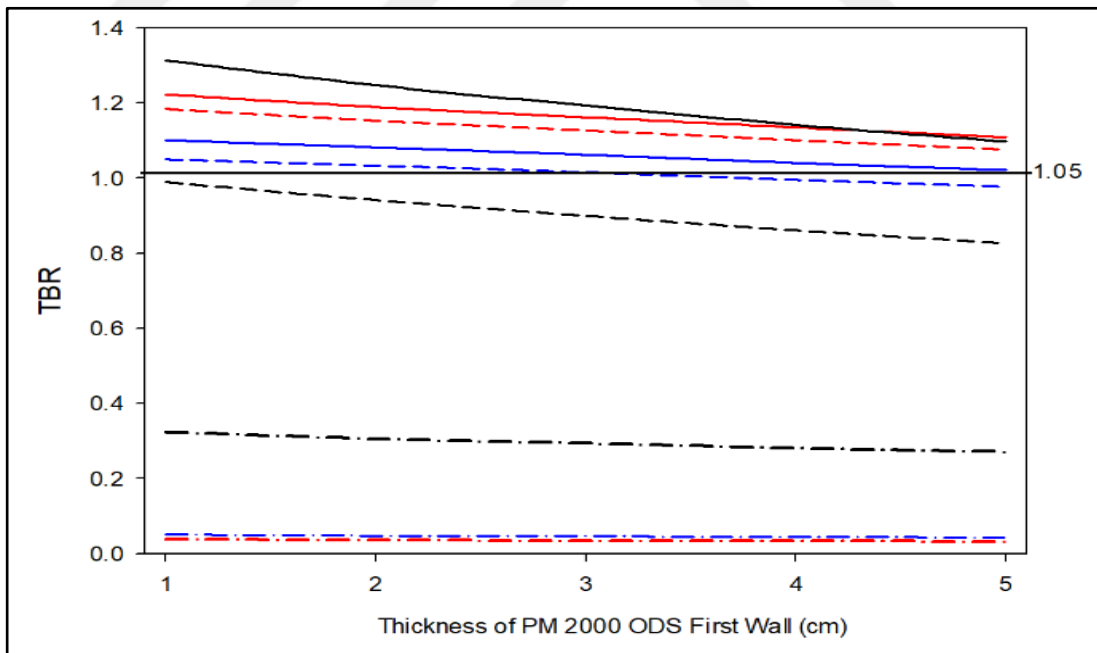


Figure 4.4. The Change of Tritium Breeding Ratio with respect to Thickness for PM2000 ODS Steel Alloy First Wall Materials (given separately in the coolant zone and the tritium breeding zone).

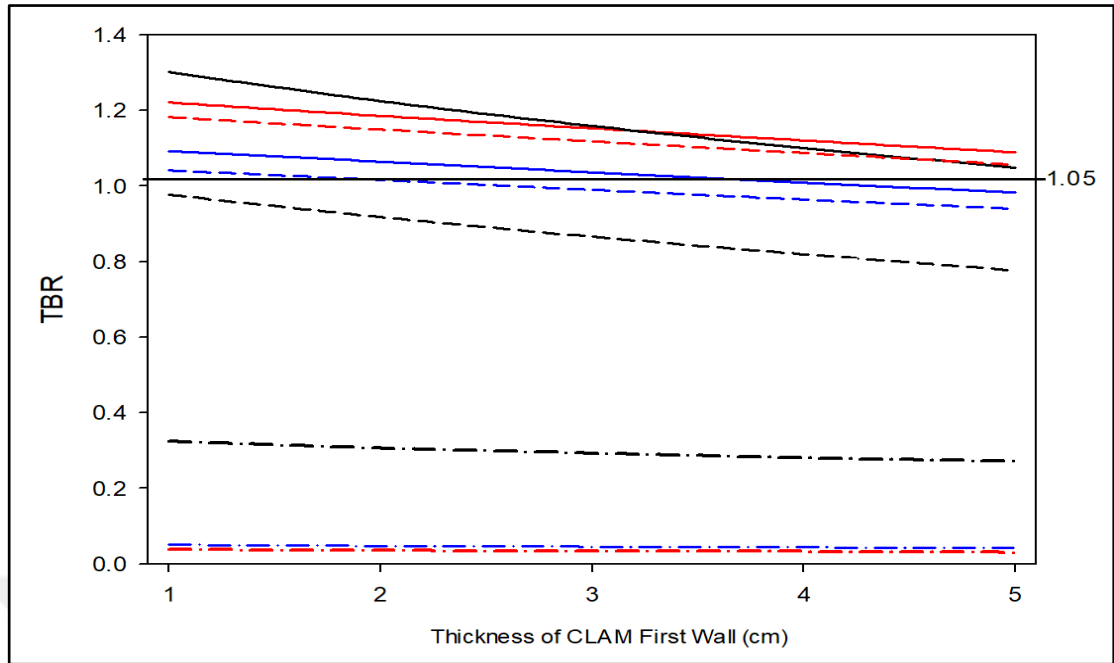


Figure 4.5. The Change in Tritium Breeding Ratio with respect to Thickness for CLAM Steel Alloy First Wall Materials (given separately in the coolant zone and the tritium breeding zone).

As can be seen from the Figure 4.6., in the first wall material (SS 316 LN-IG), the TBR values decrease from 1.20 to 1.00, from 1.28 to 1.00 and from 1.08 to 0.94 for FLiBe coolant, FLiPb coolant and FLiNaBe coolant, respectively, as the first wall material thickens from 1 cm to 5 cm. When these values are examined for the first wall material (SS 316 LN-IG), the highest reduction in TBR was 21% for FLiBe coolant. In the same examination in Figure 4.7., in the first wall material (PM2000 ODS), the TBR values decrease from 1.22 to 1.10, from 1.31 to 1.09 and from 1.10 to 1.02 for FLiBe coolant, FLiPb coolant and FLiNaBe coolant, respectively, as the first wall material thickens from 1 cm to 5 cm. When these values are examined for the first wall material (SS 316 LN-IG), the highest reduction in TBR was 16% for FLiBe coolant. For the first wall material (CLAM) in Figure 4.8., the TBR values decrease from 1.22 to 1.08, from 1.30 to 1.04 and from 1.09 to 0.98 for FLiBe coolant, FLiPb coolant and FLiNaBe coolant, respectively, as the first wall material thickens from 1 cm to 5 cm. When these values are examined for the first wall material (SS 316 LN-IG), the highest reduction in TBR was 20% for FLiBe coolant. In terms of TBR, the best performance was obtained for 1 cm first wall material Stainless Steel (PM2000 ODS).

Sufficient tritium production in the fusion reactor blanket must be maintained to sustain the fusion reactor. Figures are useful to evaluate how the first wall thickness will affect the overall tritium production.

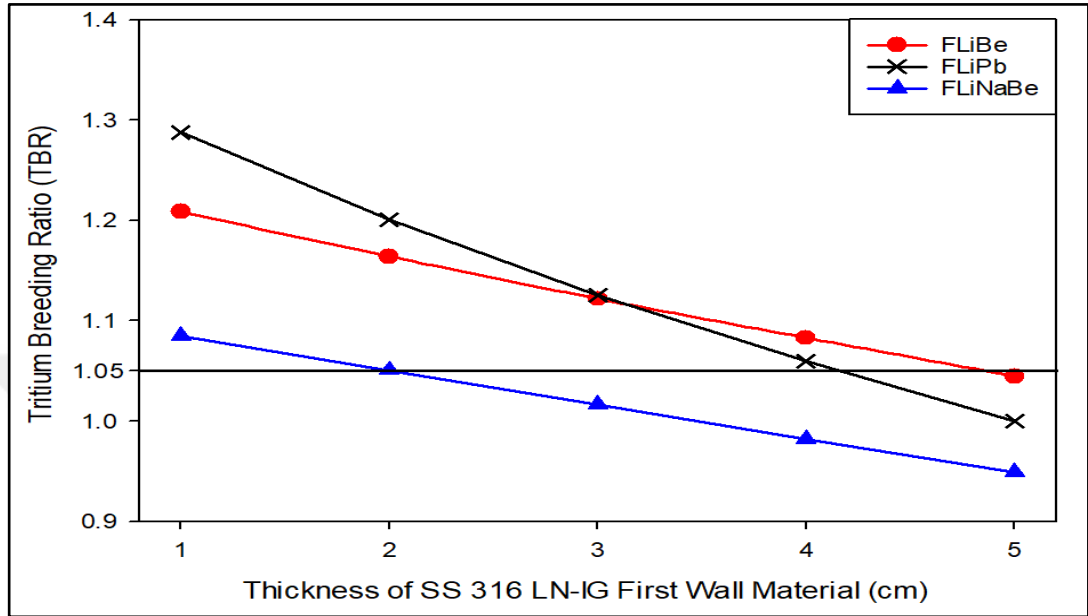


Figure 4.6. The Change in the Tritium Breeding Ratio with respect to Thickness for SS 316 LN-IG Steel Alloy First Wall Materials.

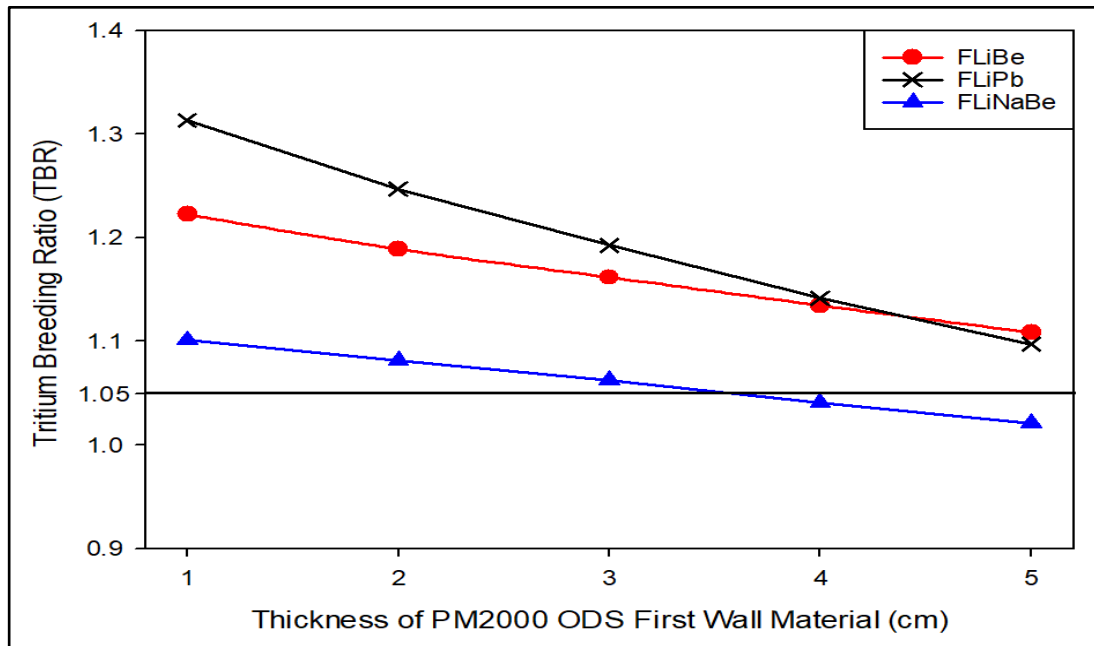


Figure 4.7. The Change in the Tritium Breeding Ratio with respect to Thickness for PM2000 ODS Steel Alloy First Wall Materials.

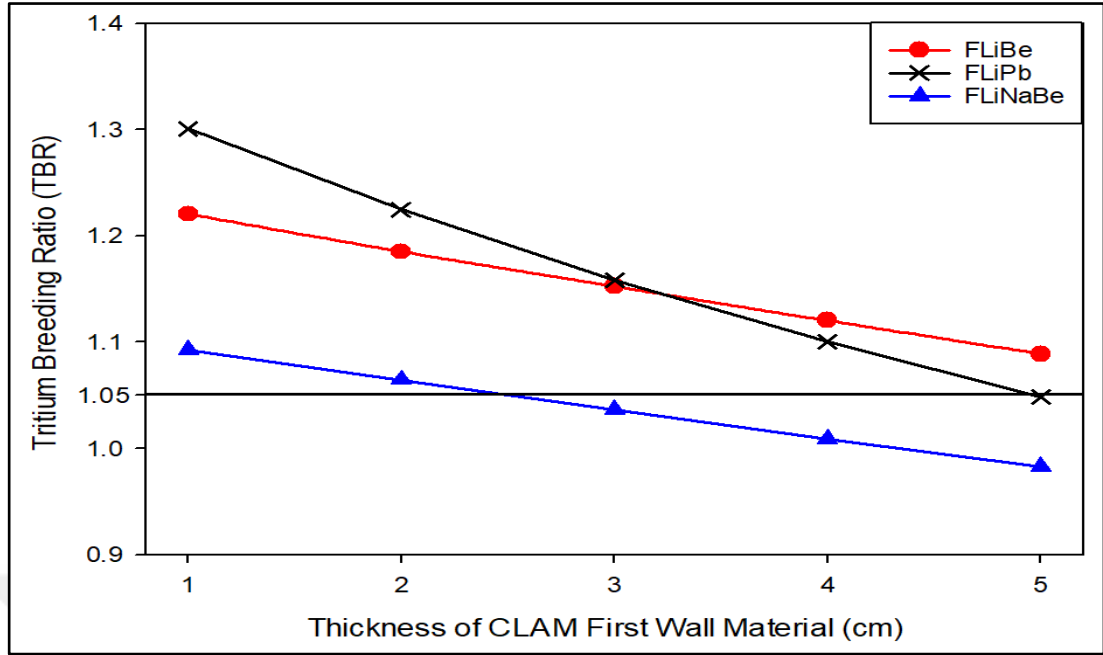


Figure 4.8. The Change in the Tritium Breeding Ratio with respect to Thickness for CLAM Steel Alloy First Wall Materials

#### 4.1.2. Energy Multiplication Factor

Energy multiplication through various neutronic reactions in the blanket is an important performance parameter of a fusion reactor. In the blanket of a fusion reactor, nearly all the kinetic energy of 14 MeV neutrons is converted into useful heat energy by multiple scattering.

The multiplication factor (M) was calculated using Equation 4.3.

$$M = 1 + \frac{(\Sigma_{\text{tritium}}({}^6\text{Li}) \times 4.786) - (\Sigma_{\text{tritium}}({}^7\text{Li}) \times 2.467) \text{ MeV}}{14.1 \text{ MeV}} \quad (4.3)$$

Per Equation (1), the exoenergetic neutron absorption in  ${}^6\text{Li}$  occur the tritium breeding and the important effect of heat generation in the coolant and tritium breeding zones. In addition, the addition of neutron multiplier  $\text{Be}(n,2n)$  and  $\text{Pb}(n,2n)$  to the coolant increases the energy multiplication factor. Moreover, the  $\gamma$ -emissions in the first wall material and coolants resulting from the  $(n, \gamma)$  reactions contribute to the overall heat energy production. Figure 4. 9., Figure 4.10. and Figure 4.11. show the change of

multiplication factor (M) with respect to thickness for first wall materials and coolants. The highest energy multiplication is observed with the FLiPb coolant, which is directly related to the neutron multiplier and the intense  $\gamma$  emission in lead and occurs via multiple inelastic neutrons scattering reactions. As shown in the Figure 4.6., Figure 4.7. and Figure 4.8. and Figure 4. 9., Figure 4.10. and Figure 4.11., both M factor and TBR are the highest due to neutron multiplication in the FLiPb coolant, additionally M and TBR values decrease as the thickness for first wall materials increases.

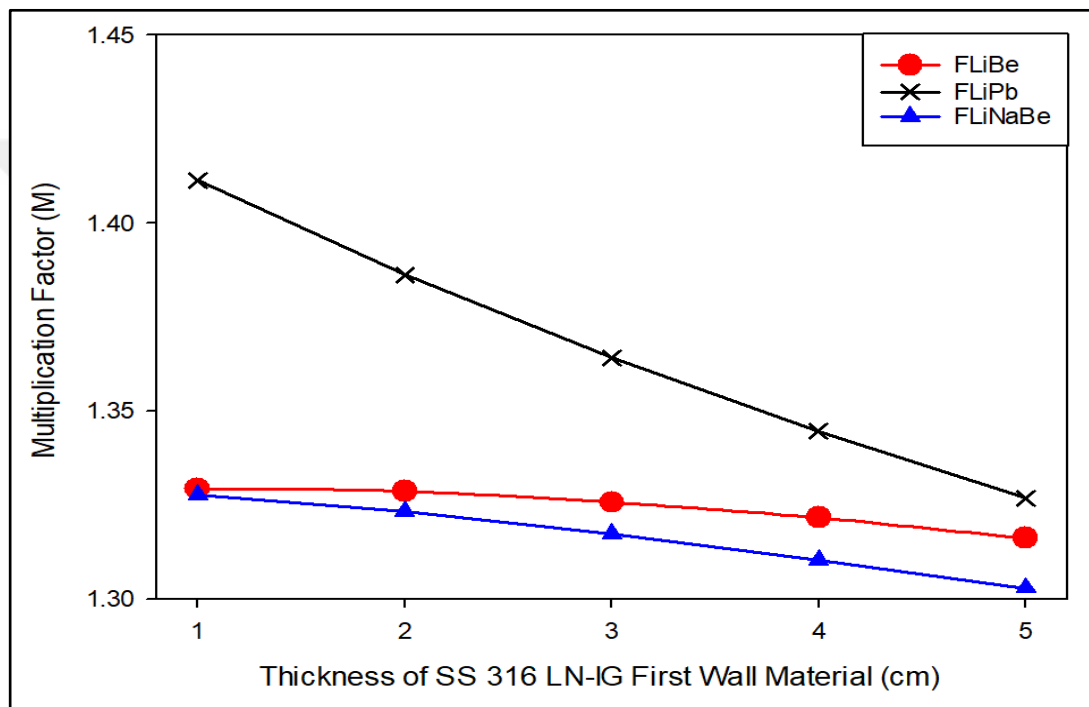


Figure 4.9. The Change in the Multiplication Factor with respect to Thickness for SS 316 LN-IG Steel Alloy First Wall Materials and Coolants

## 4.2. RADIATION DAMAGE IN THE FIRST WALL

In a fusion reactor, the first wall (FW) is exposed to large amounts of plasma particles and electromagnetic radiation. At the same time, the first wall protects the blanket from plasma. Additionally, the first wall (FW) is exposed to 14 MeV high-energy neutrons released from the DT reaction. High energy neutrons cause nuclear reactions in the first wall in terms of material damage, a criterion of the fusion reactor structural, it is known that the most important parameters are DPA, gas production such as Helium and Hydrogen production.

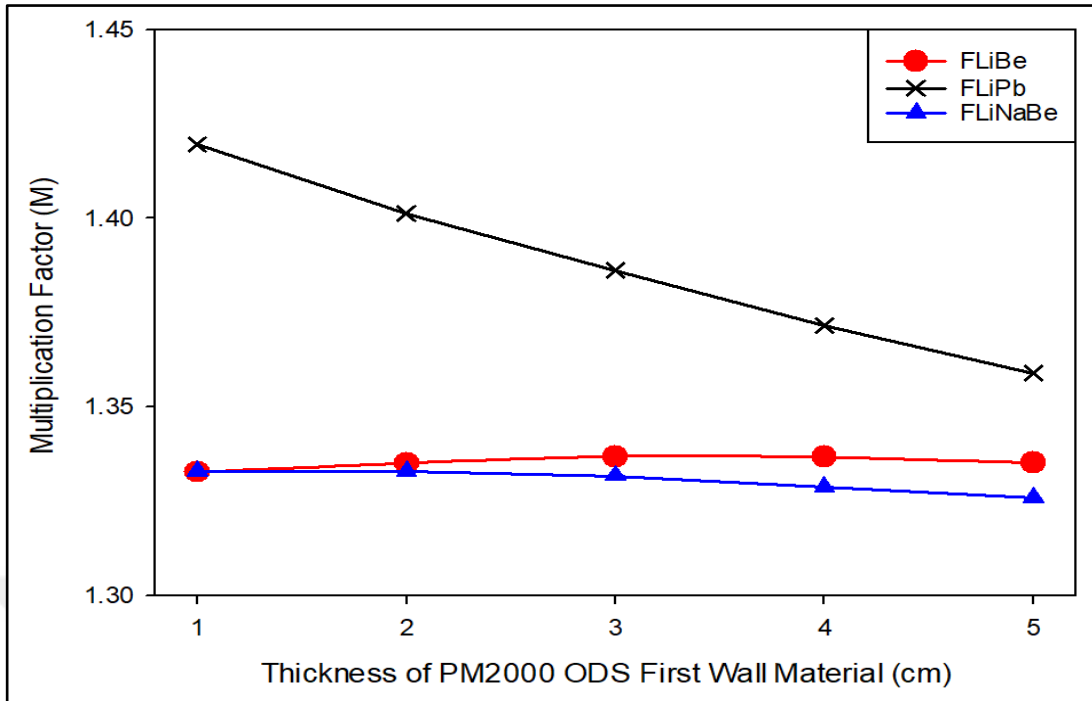


Figure 4.10. The Change in the Multiplication Factor with respect to Thickness for PM2000 ODS Steel Alloy First Wall Materials and Coolants

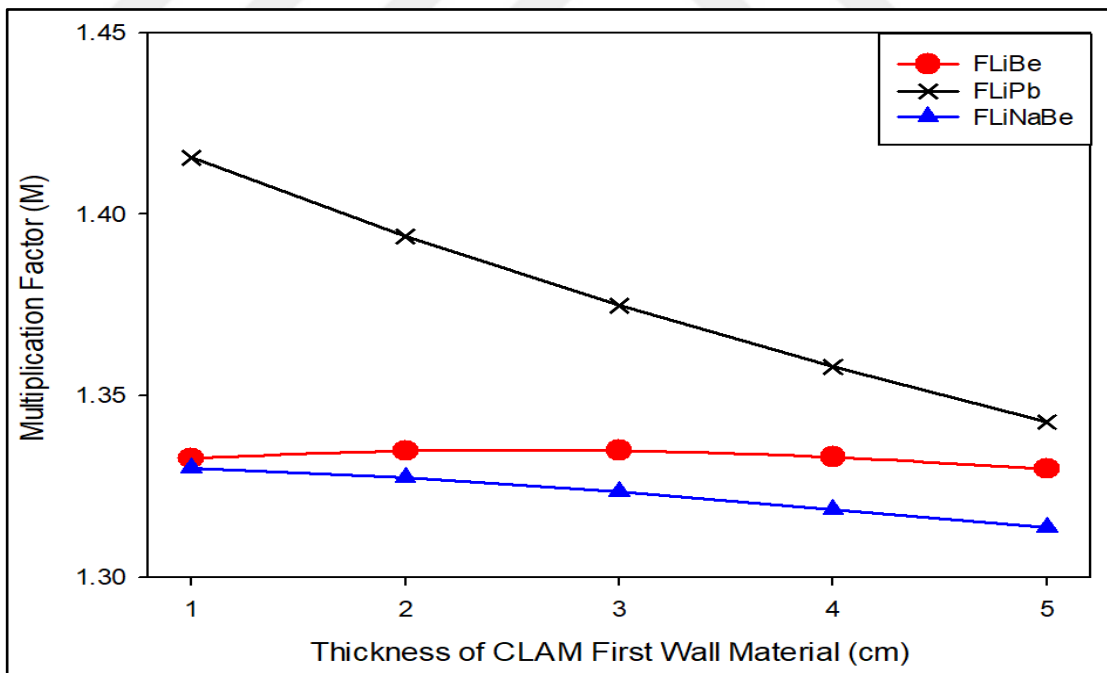


Figure 4.11. The Change in the Multiplication Factor with respect to Thickness for CLAM Steel Alloy First Wall Materials and Coolants

Radiation damage, a design concept for fusion energy reactors, limits the lifetime for the FW structure to 1 Full Power Year (FPY), meaning that the FW material must be replaced every year. In this study, a DPA limit criteria of the FW structural materials is selected 100 DPA/FPY [44,45]. Radiation damage beyond certain limits causes the first wall materials to be replaced. In addition, the acceptable limit for Helium production has been chosen 500 appm (atomic parts per million) according to literature [46,47]. When First Wall radiation is evaluated in terms of damage criteria, it is seen that the first wall thicknesses used in this study are sufficient. However, when evaluated in terms of the Fusion reactor Blanket as a whole, it is seen that the FLiBe and FLiPb coolant, in which ODS steel are used together, give the best performance, especially when TBR production is considered seen in Figure 4. 6., Figure 4.7. and Figure 4.8.

#### **4.2.1. Displacement Per Atom**

Displacement per atom (DPA) is expressed as a measure of the damage caused to the atomic crystal structure of a substance by bombardment with energetic particles. In other words, the number of times each atom is separated from its place in the crystal by radiation. The displacement per atom in a lattice structure is called DPA. In other words, 1 DPA is equivalent to displacing all atoms once from their lattice sites. In the first wall calculations, the displacement per atom is expressed as a probability. This possibility is called the DPA cross section. The neutrons that cause DPA are usually neutrons with an energy greater than 1 MeV. Thermal neutrons do not cause DPA. The cross-section for processes of neutron displacement damage is generally in the range from 1 to 10 barns [42].

The three types of first wall material were considered for first wall performance. However, also coolants behind the first wall affect the structure of the first wall. Because the coolants contain neutron multiplier isotopes. Thus, both factors should take into consideration the evaluation of the DPA performance. It can be seen in Figure 4.12., Figure 4.13. and Figure 4.14. the first wall damage (DPA) is higher when FLiPb coolant is used since high energy neutrons (14 MeV) have a higher Pb(n,2n) cross section and high neutron multiplier. Namely, as the number of neutrons in the material

increases, more DPA occurs on the first wall than FLiBe coolant and FLiNaBe coolant. In addition, since Fe and Cr elements are in the highest content of all the first wall materials, one can say that the DPA damages of the first wall materials are approximately similar.

The change of the DPA values with respect to thickness for first wall materials and three different coolants is shown in Figure 4.12., Figure 4.13. and Figure 4.14. The neutron moderation in Lithium, the lightest coolant element decreases DPA, also seen in CLAW-IV library. Neutron multiplication in FLiPb is higher than Neutron multiplication in FLiBe and FLiNaBe because high energy neutrons (14 MeV) have a higher cross-section of Pb(n,2n), whereas thermal neutrons have a higher cross-section of Be(n,2n). Therefore, it can be observed in **Figure 4.12.**, the lead containing FLiPb coolant has the highest DPA values for the first wall materials. In the first wall material (SS 316 LN-IG), the DPA values decrease from 7.17 to 5.66, from 7.95 to 6.09 and from 7.18 to 5.69 for FLiBe coolant, FLiPb coolant and FLiNaBe coolant, respectively, as the first wall material thickens from 1 cm to 5 cm. When these values are examined for the first wall material (SS 316 LN-IG) in Figure 4.13., the highest reduction in DPA was 23% for FLiPb coolant. In the same examination, in the first wall material (PM2000 ODS), the DPA values decreases from 7.26 to 5.86, from 8.05 to 6.32 and from 7.27 to 5.89 for FLiBe coolant, FLiPb coolant and FLiNaBe coolant, respectively, as the first wall material thickens from 1 cm to 5 cm. When these values are examined for the first wall material (SS 316 LN-IG), the highest reduction in DPA was 21% for FLiPb coolant. For the first wall material (CLAM) in Figure 4.14. the DPA values decrease from 7.12 to 5.68, from 7.83 to 6.12 and from 7.14 to 5.71 for FLiBe coolant, FLiPb coolant and FLiNaBe coolant, respectively, as the first wall material thickens from 1 cm to 5 cm. When these values are examined for the first wall material (SS 316 LN-IG), the highest reduction in DPA was 22% for FLiPb coolant.

#### **4.2.2. Gas Production**

Due to higher  $\sigma(n,p)$  cross-section than  $\sigma(n,\alpha)$  and lower (n,p) threshold energies than (n, $\alpha$ ) threshold energies, higher H production than He production was obtained for the investigated FW structures [48].

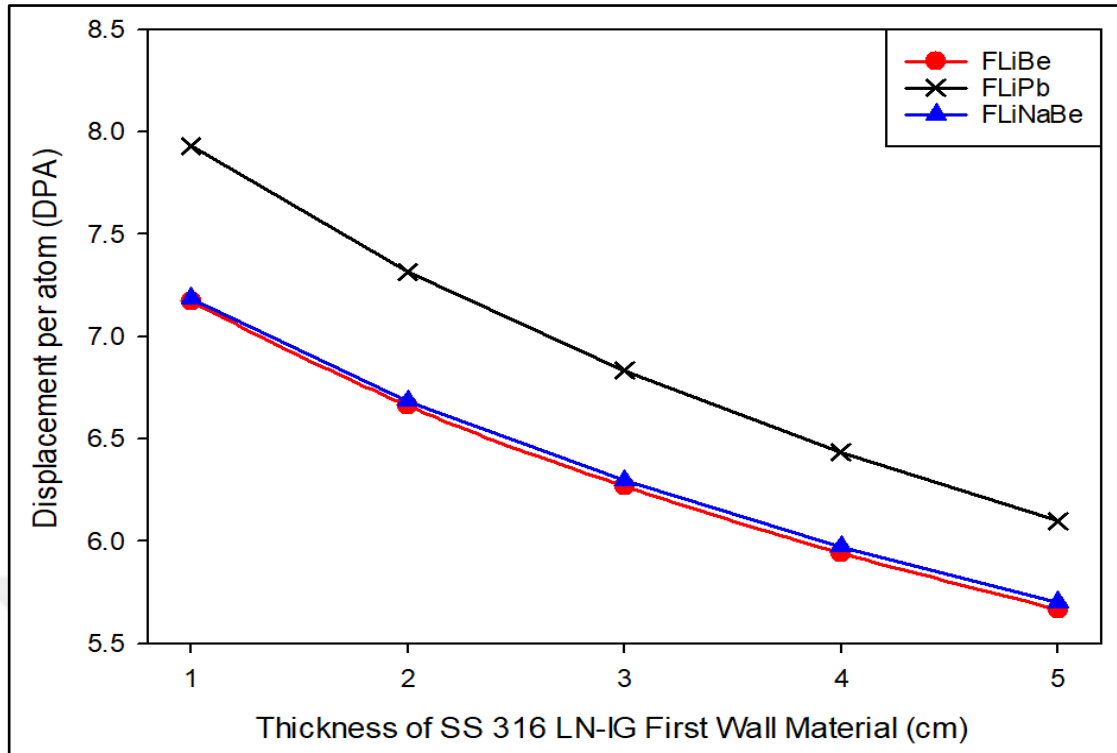


Figure 4.12. The Change in the Displacement per Atom with respect to Thickness for SS 316 LN-IG Steel Alloy First Wall Materials.

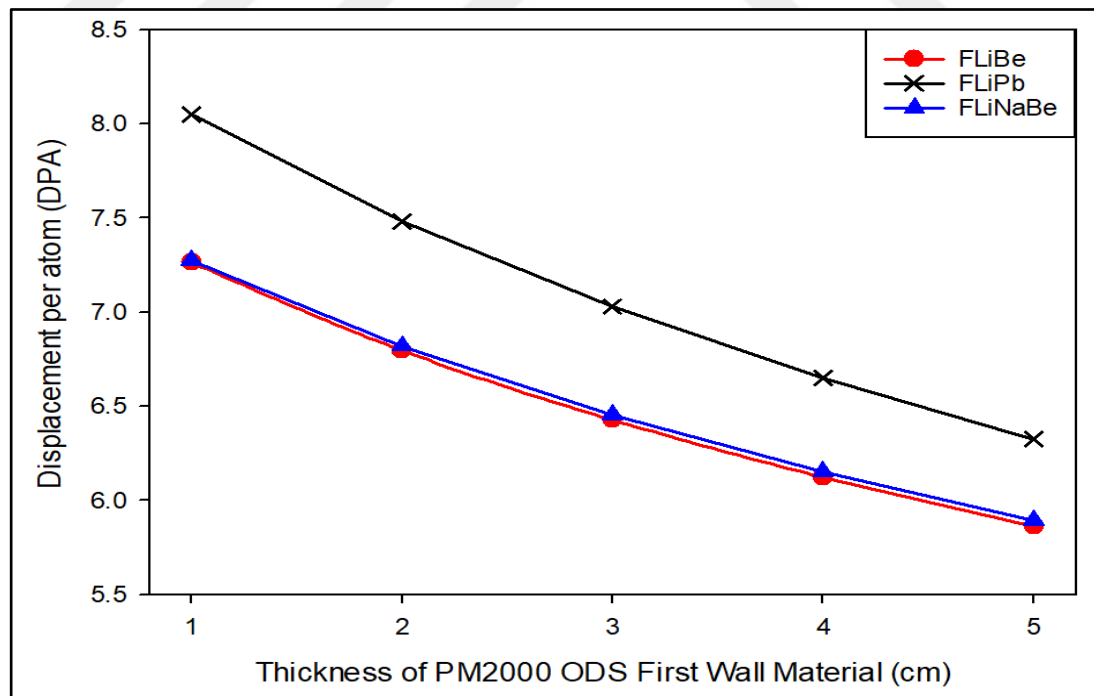


Figure 4.13. The Change in the Displacement per Atom with respect to Thickness for PM2000 ODS Steel Alloy First Wall Materials.

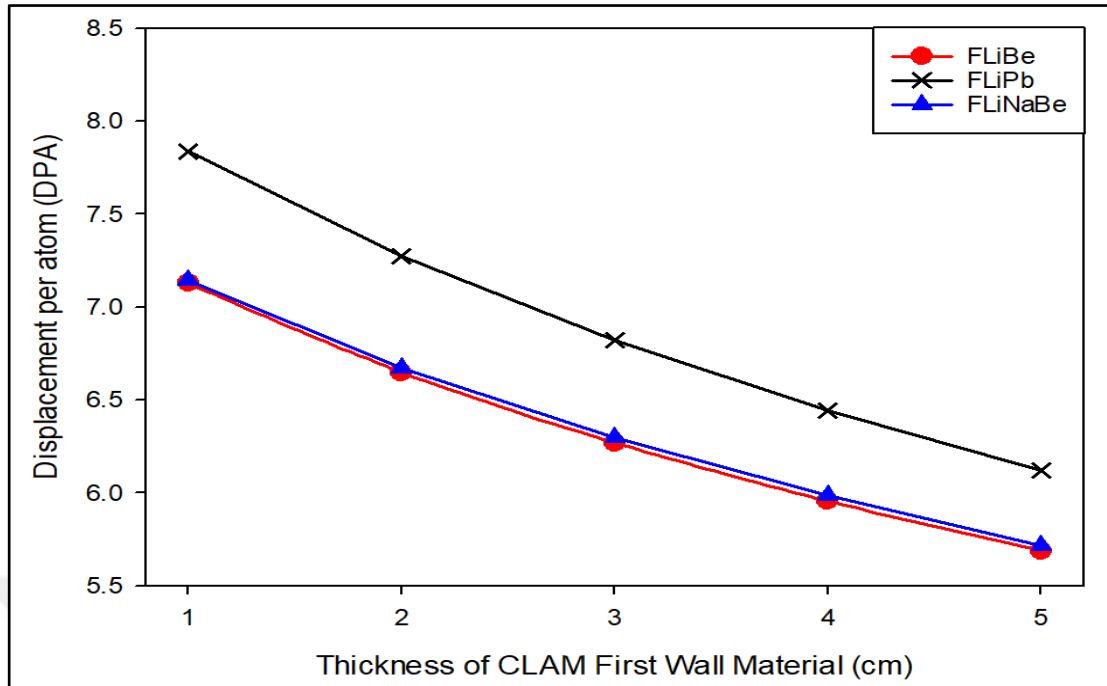


Figure 4.14. The Change in the Displacement per Atom with respect to Thickness for CLAM Steel Alloy First Wall Materials.

Figure 4.15., Figure 4.16. and Figure 4.17. show the change of Hydrogen (H) production with respect to thickness of the first wall materials, and the H-production decreases as the material thickness increases moreover having the approximately same values per full power year for all first wall materials. When the overall Figure 4.15., Figure 4.16. and Figure 4.17. are examined, the lowest H-production values were obtained for FLiPb coolant, the highest H-production values were obtained for FLiBe and FLiNaBe coolants, which are almost same H-production values. It is seen in the overall Figure 4.15., Figure 4.16. and Figure 4.17. that the values obtained for FLiBe and FLiNaBe coolants are slightly above these values. The highest same H-production values were from 219.2, 175.1 and 179.5 appm/FPW to 140.3, 114.6 and 116.2 appm/FPW using FLiBe and FLiNaBe coolant for SS316, ODS and CLAM, respectively, reductions in H-production value were the same as 35%. Since all the hydrogen isotopes produced by the (n, p), (n, d), (n, t) reactions will diffuse out of the metallic lattice or form metal hybrids, H-production values were not taken into consideration in this study. Therefore, no damage limit was chosen for H-production in the is study.

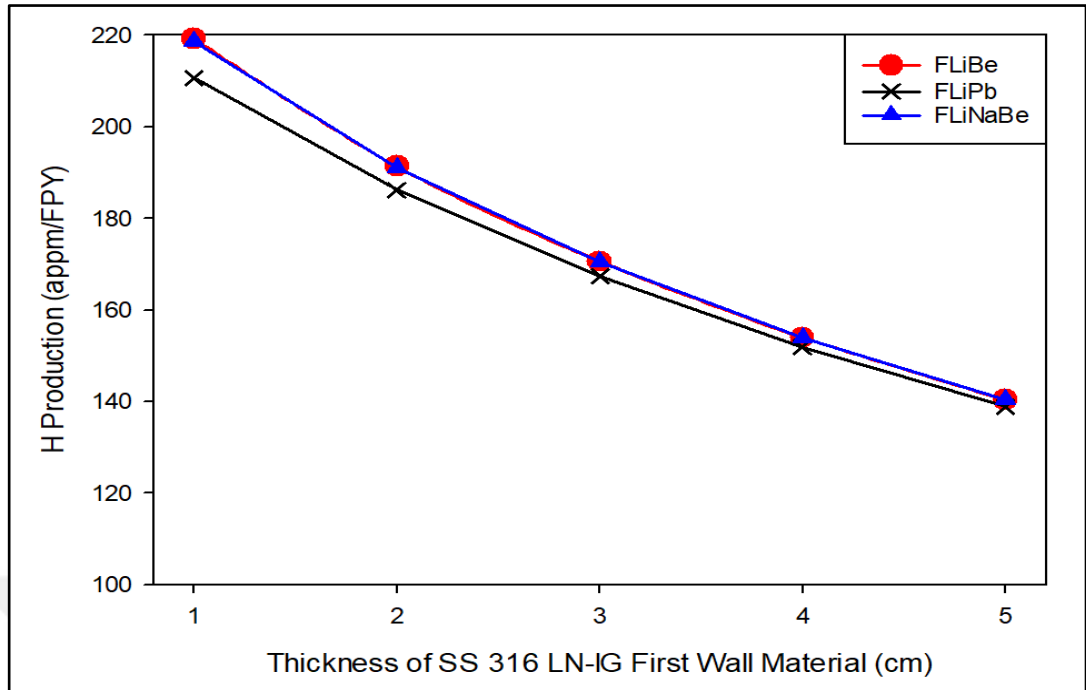


Figure 4.15. The Change in Hydrogen Production with respect to Thickness for SS 316 LN-IG Steel Alloy First Wall Materials.

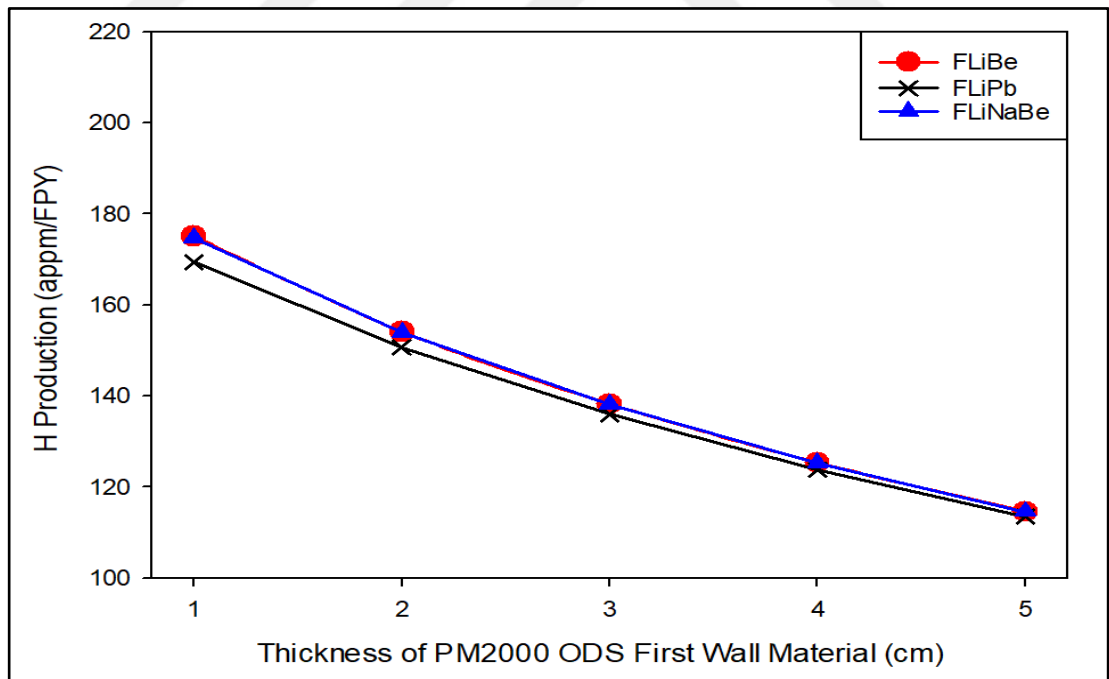


Figure 4.16. The Change in Hydrogen Production with respect to Thickness for PM2000 ODS Steel Alloy First Wall Materials.

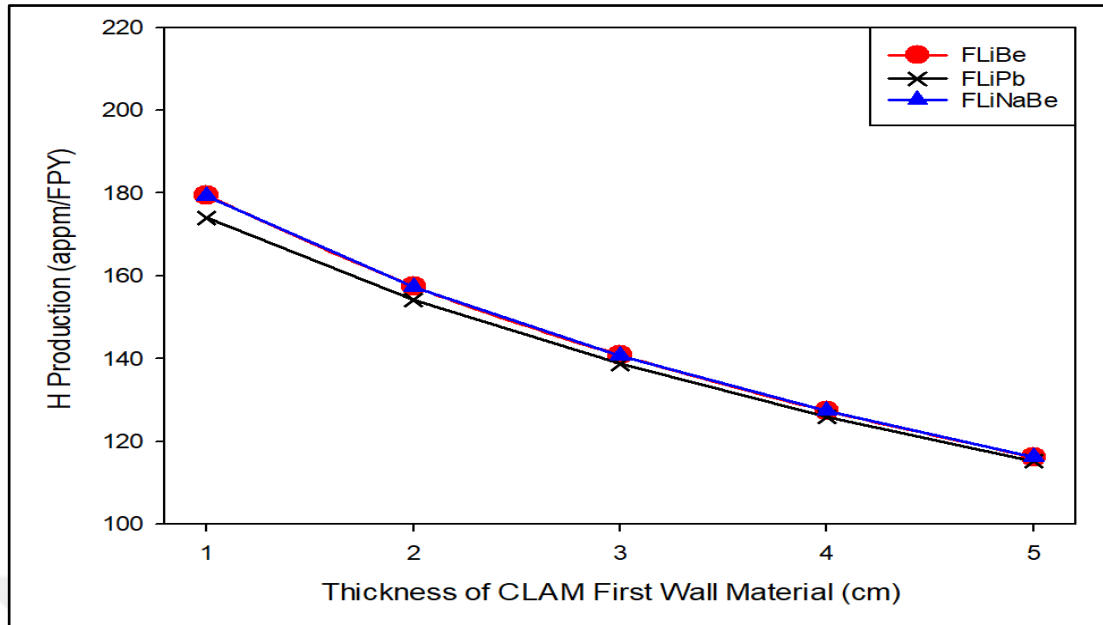


Figure 4.17. The Change in Hydrogen Production with respect to Thickness for CLAM Steel Alloy First Wall Materials.

Figure 4.18., Figure 4.19. and Figure 4.20. show the change of Helium (He) production with respect to thickness of the first wall and coolant materials, and the He-production decreases as the material thickness increases moreover having the approximately same values per full power year for all first wall materials. The same situation can be seen when the overall Figure 4.18., Figure 4.19. and Figure 4.20. are examined, the lowest He-production values were obtained for FLiPb coolant, the highest He-production values were obtained almost same for FLiBe and FLiNaBe coolants. FLiBe and FLiNaBe coolants are slightly above these values. They decrease slowly from 83.5, 81.7 and 69.3 appm/FPW to 53.1, 53.3 and 44.7 appm/FPW using FLiBe and FLiNaBe coolant for SS316, ODS and CLAM, respectively.

As clearly observed from Figure 4.15., Figure 4.16. and Figure 4.17. and Figure 4.18., Figure 4.19. and Figure 4.20., H-production is significantly higher than He-production, related to lower threshold energy and higher hydrogen cross-sections.

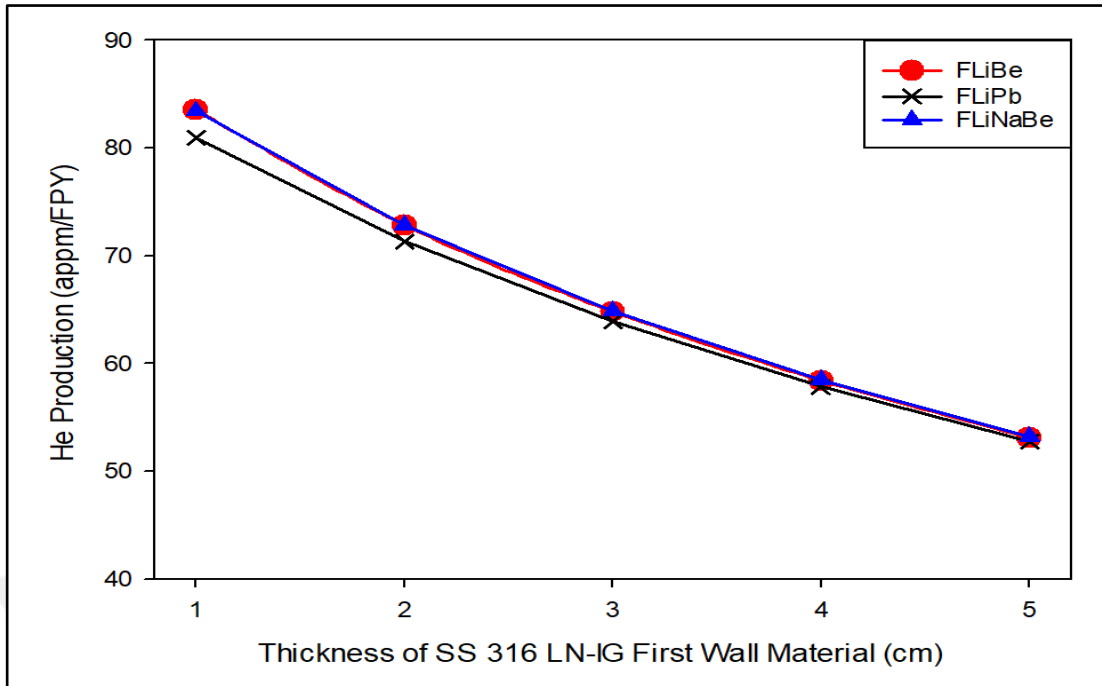


Figure 4.18. The Change in Helium Production with respect to Thickness for SS 316 LN-IG Steel Alloy First Wall Materials.

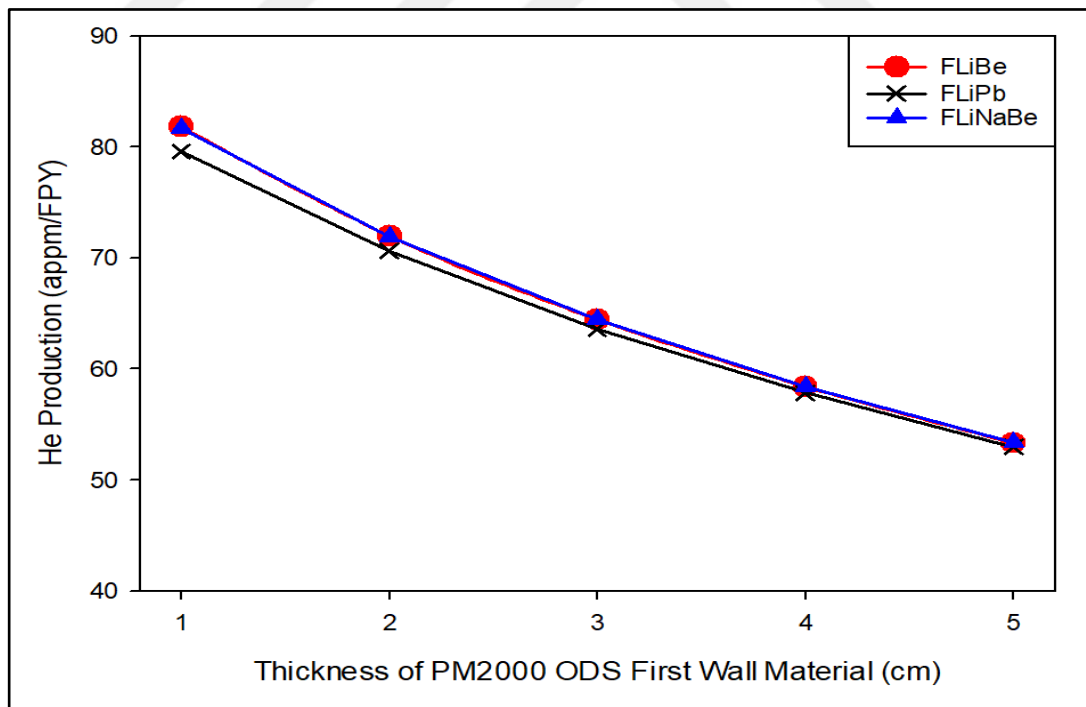


Figure 4.19. The Change in Helium Production with respect to Thickness for PM2000 ODS Steel Alloy First Wall Materials.

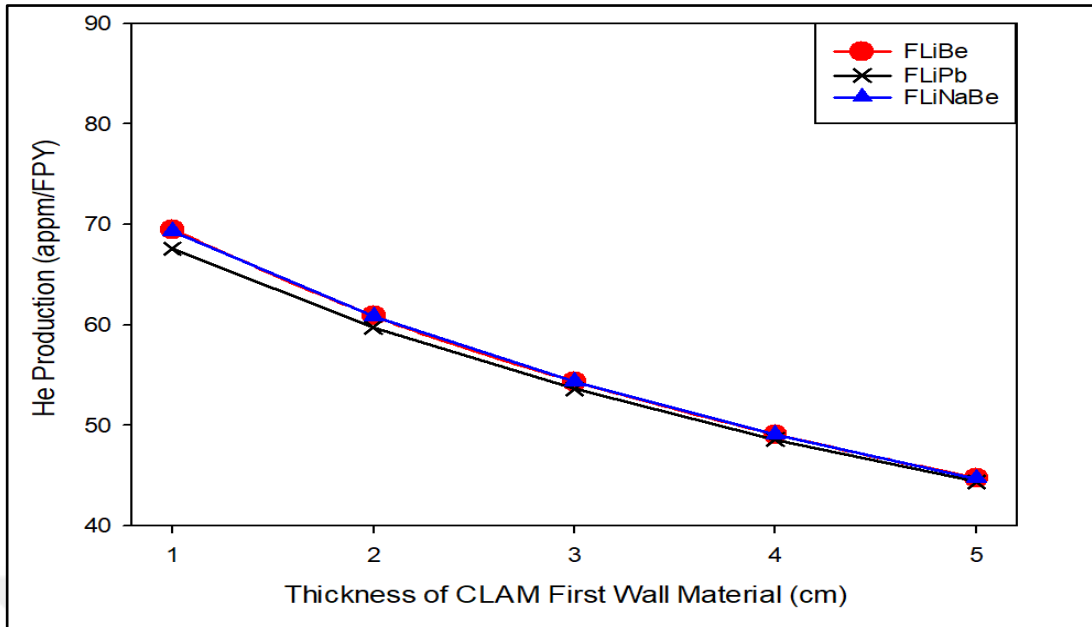


Figure 4.20. The Change in Helium Production with respect to Thickness for CLAM Steel Alloy First Wall Materials.

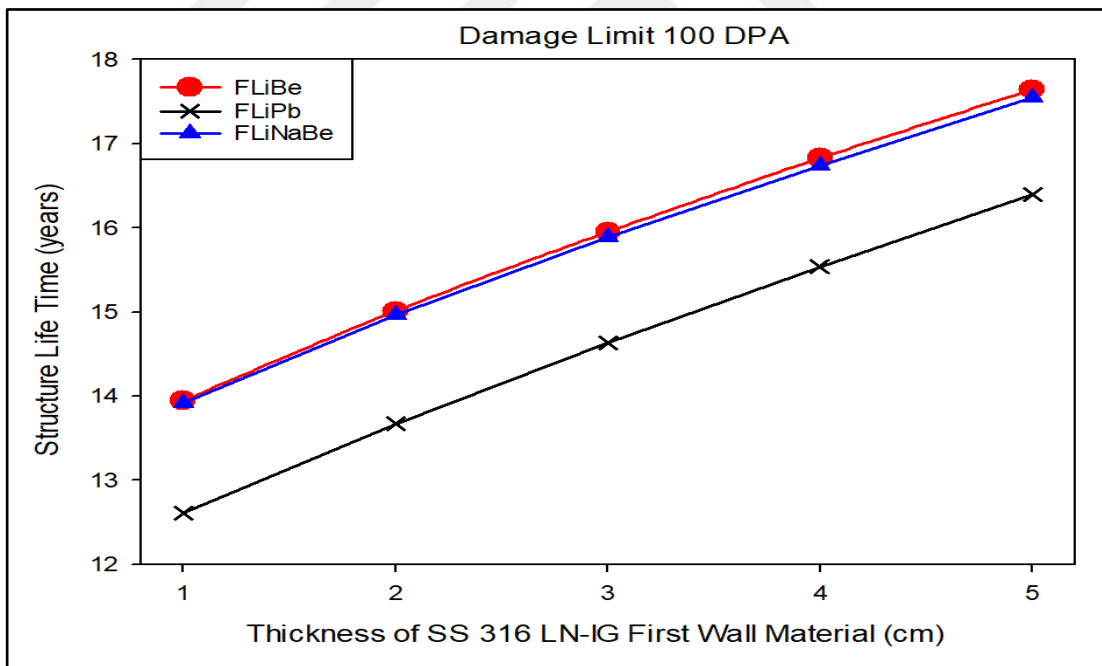


Figure 4.21. The Change in Structural Lifetime with respect to Thickness for SS 316 LN-IG Steel Alloy First Wall Materials Regarding the DPA Limit

### 4.2.3. Structural Lifetime

The determining time for replacement of the first wall is known as the DPA breakpoint. In the literature, many studies have been done between DPA value 100 and 1000 atomic particles per million (appm) as the design limit for candidate structural materials [46,47,49-52]. According to all these references, a more conservative limit of 100 DPA has been applied for radiation damage in this study. Figure 4.21., Figure 4.22. and Figure 4.23. show DPA values for the investigated FW structural materials thickness and three different coolants as a function of the years. When Figure 4.21., Figure 4.22. and Figure 4.23. are examined in overall regarding the DPA limit, the lowest lifetime with FLiPb coolant was achieved DPA damage. DPA damages start from 12.6, 12.4 and 12.7 years to 16.3, 15.8 and 16.3 years with FLiBe, SS-316, ODS and CLAM structure, respectively, as the first wall material thickens from 1 to 5 cm.

Besides, the  $\alpha$ -particles ( $n, \alpha$ ) will remain in metal and produce bubbles of helium gas, i.e. He-production. A conservative design limit of He-production has been suggested 500 atomic parts per million [appm] as criteria for helium production in the FW structure in this study. Figure 4.24., Figure 4.25. and Figure 4.26. show the change of structural lifetime with respect to thickness for first wall materials with three different coolants regarding He-production limit. As seen in Figure 4.24., Figure 4.25. and Figure 4.26., almost the same lifetime values are observed. These replacement periods are from 6 years to 11 years.

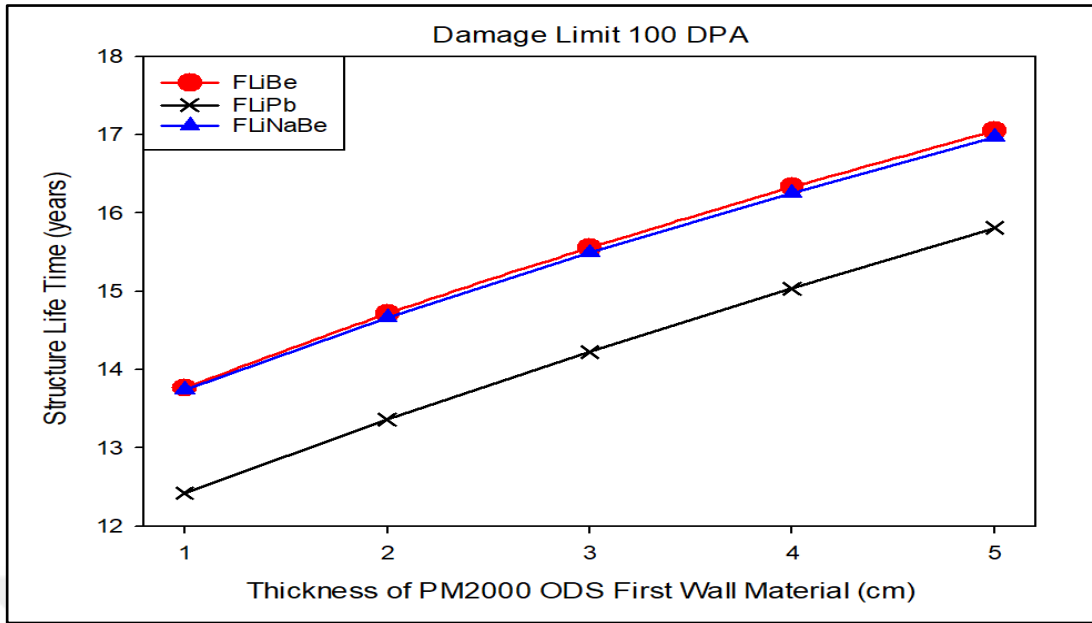


Figure 4.22. The Change in Structural Lifetime with respect to Thickness for PM2000 ODS Steel Alloy First Wall Materials Regarding the DPA Limit.

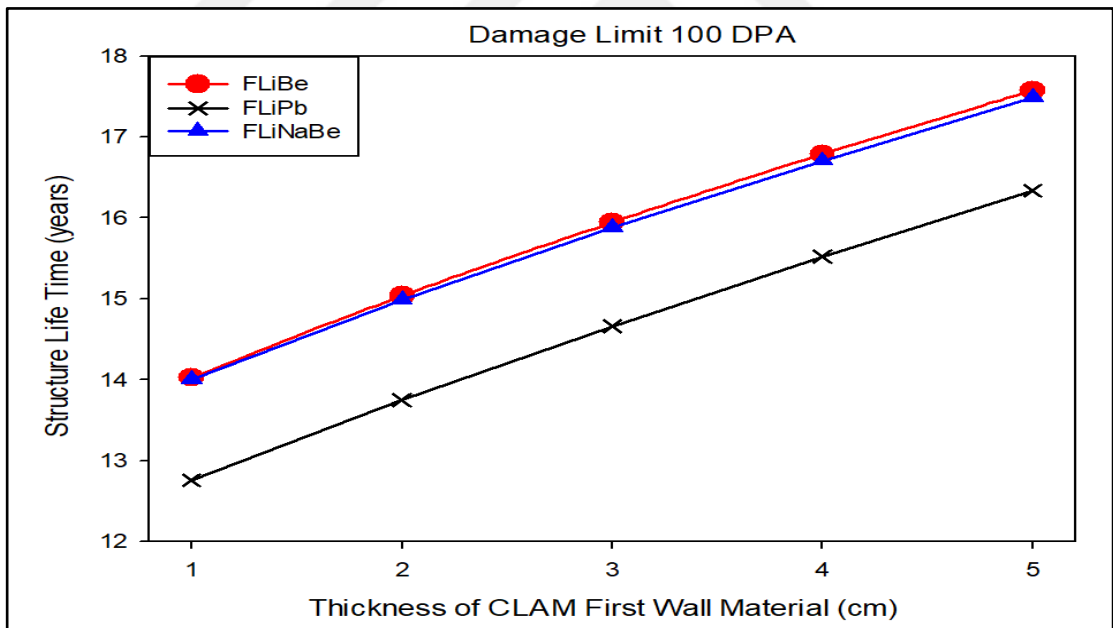


Figure 4.23. The Change in Structural Lifetime with respect to Thickness for CLAM Steel Alloy First Wall Materials Regarding the DPA Limit.

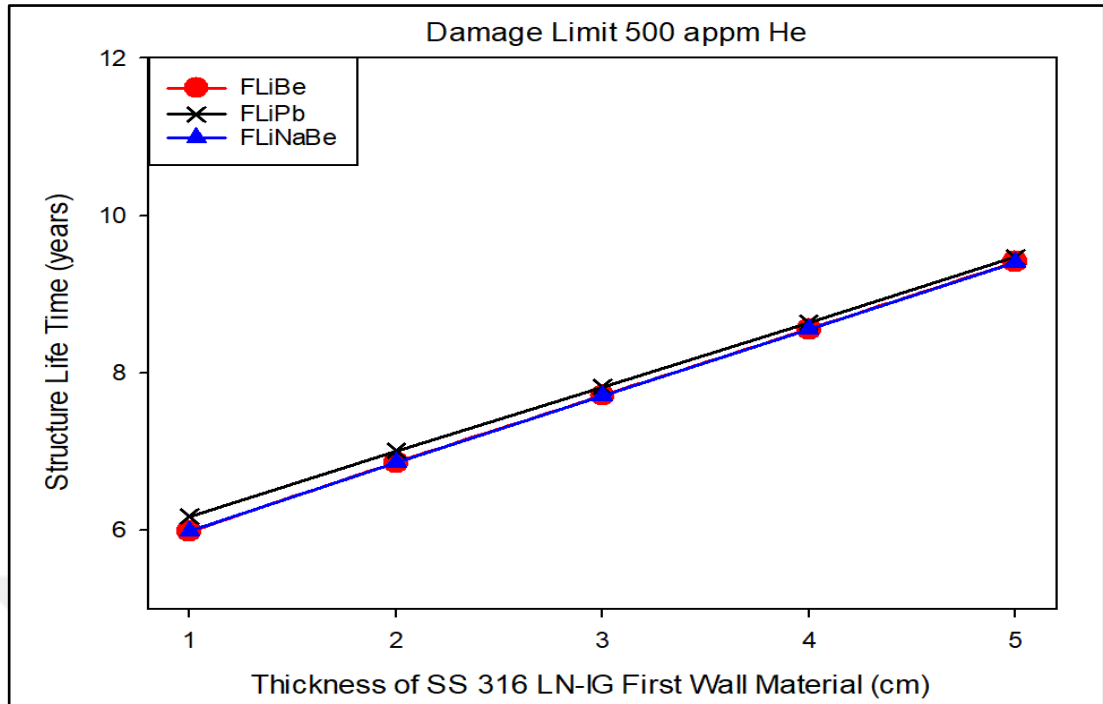


Figure 4.24. The Change in Structural Lifetime with respect to Thickness for SS 316 LN-IG Steel Alloy First Wall Materials Regarding He Limit.

The Helium to DPA ratio (He/DPA) determines whether the damage to the first wall is primarily due to DPA or helium production. This value will be 5 as the limit value for Helium is 500 appm and for DPA the limit value is 100 appm. If the He/DPA value is less than 5, DPA is first, and if it is greater than five, He production starts to do damage first. When Table 4. 1. is examined, it is seen that the He/DPA ratio is above 5 in all FW materials and all molten salt coolants. In addition, DPA and He structural lifetime and He/DPA ratio with respect to different first wall materials and coolants can be figured out. Moreover, the overall seen in Table 4. 1., differs from DPA damage meaning leads to the highest helium production and gas bubbles built in metallic crystal for all FW materials. In the light of all these explanations, He- production should be considered as the factor determining the replacement of FW material in this study.

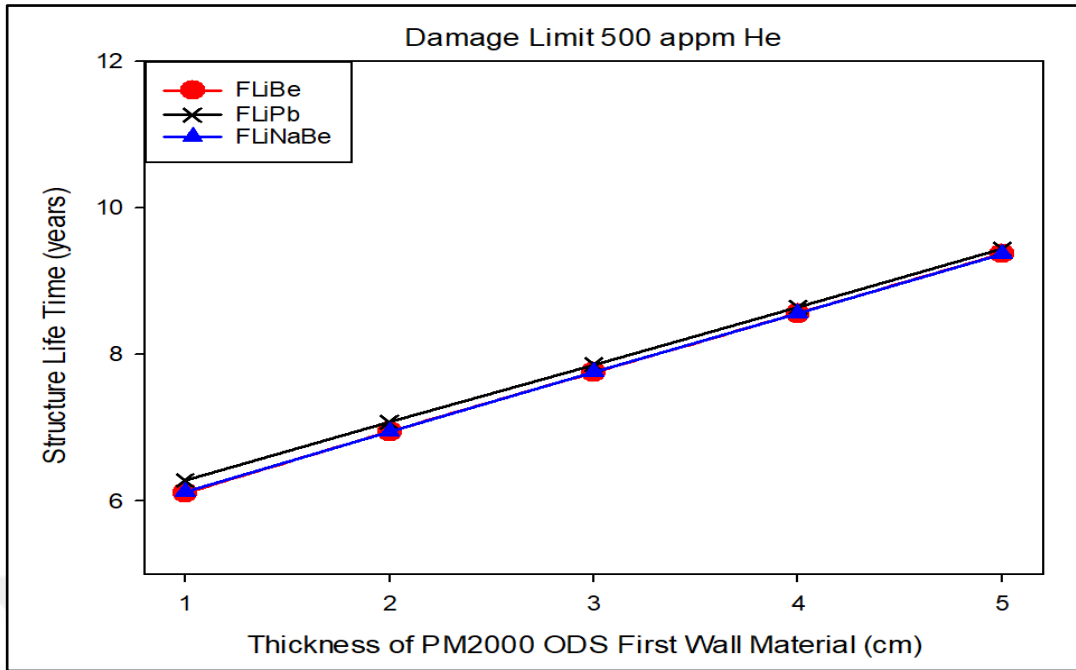


Figure 4.25. The Change in Structural Lifetime with respect to Thickness for PM2000 ODS Steel Alloy First Wall Materials Regarding He Limit.

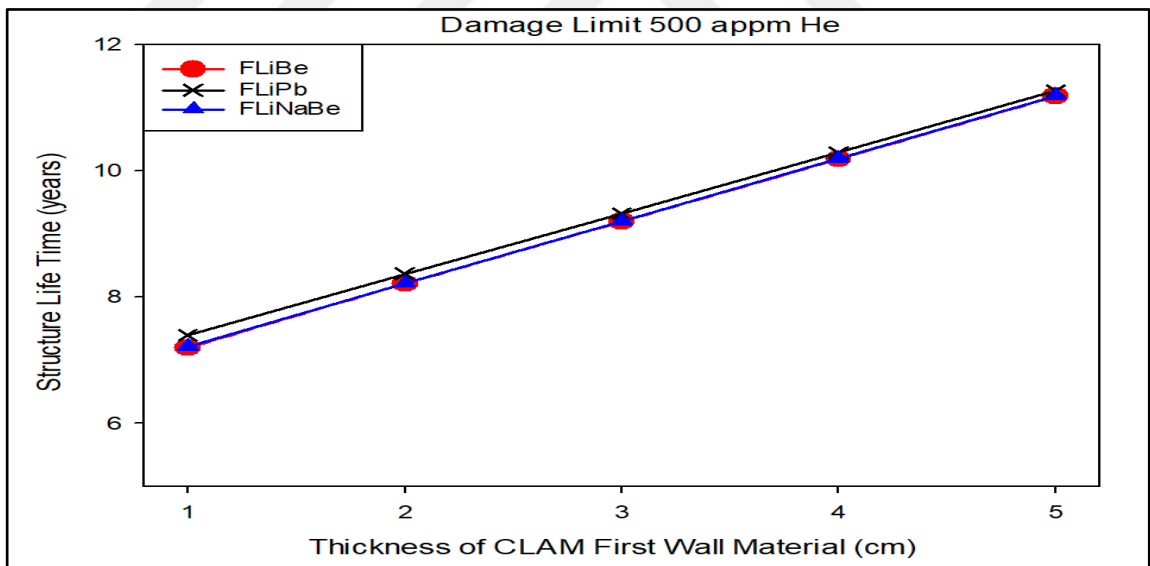


Figure 4.26. The Change in Structural Lifetime with respect to Thickness for CLAM Steel Alloy First Wall Materials Regarding He Limit.

Table 4.1. DPA and He Structural Lifetime and He/DPA ratio with respect to Different First Wall Materials and Coolants.

| First Wall \ Coolants | DPA-Lifetime (Year) |        |         | He-Lifetime (Year) |        |         | He/DPA |        |         |
|-----------------------|---------------------|--------|---------|--------------------|--------|---------|--------|--------|---------|
|                       | FLiBe               | FLiPb  | FLiNaBe | FLiBe              | FLiPb  | FLiNaBe | FLiBe  | FLiPb  | FLiNaBe |
| SS 316 LN-IG (1 cm)   | 13.944              | 12.608 | 13.914  | 5.984              | 6.175  | 5.993   | 11.651 | 10.209 | 11.609  |
| SS 316 LN-IG (2 cm)   | 15.012              | 13.669 | 14.961  | 6.863              | 7.008  | 6.864   | 10.938 | 9.752  | 10.899  |
| SS 316 LN-IG (3 cm)   | 15.953              | 14.631 | 15.885  | 7.712              | 7.821  | 7.708   | 10.343 | 9.354  | 10.304  |
| SS 316 LN-IG (4 cm)   | 16.830              | 15.539 | 16.740  | 8.560              | 8.643  | 8.551   | 9.831  | 8.990  | 9.788   |
| SS 316 LN-IG (5 cm)   | 17.647              | 16.397 | 17.545  | 9.412              | 9.475  | 9.399   | 9.374  | 8.652  | 9.334   |
| PM2000 ODS (1 cm)     | 13.766              | 12.422 | 13.745  | 6.110              | 6.282  | 6.120   | 11.266 | 9.886  | 11.229  |
| PM2000 ODS (2 cm)     | 14.715              | 13.366 | 14.666  | 6.947              | 7.078  | 6.951   | 10.591 | 9.443  | 10.549  |
| PM2000 ODS (3 cm)     | 15.559              | 14.224 | 15.491  | 7.755              | 7.859  | 7.756   | 10.031 | 9.050  | 9.987   |
| PM2000 ODS (4 cm)     | 16.332              | 15.038 | 16.249  | 8.562              | 8.643  | 8.559   | 9.538  | 8.699  | 9.493   |
| PM2000 ODS (5 cm)     | 17.051              | 15.809 | 16.972  | 9.375              | 9.439  | 9.370   | 9.095  | 8.374  | 9.057   |
| CLAM (1 cm)           | 14.026              | 12.757 | 14.002  | 7.195              | 7.398  | 7.210   | 9.748  | 8.622  | 9.710   |
| CLAM (2 cm)           | 15.038              | 13.749 | 14.992  | 8.213              | 8.371  | 8.222   | 9.156  | 8.212  | 9.117   |
| CLAM (3 cm)           | 15.946              | 14.660 | 15.877  | 9.198              | 9.324  | 9.205   | 8.668  | 7.861  | 8.624   |
| CLAM (4 cm)           | 16.789              | 15.521 | 16.705  | 10.187             | 10.289 | 10.191  | 8.240  | 7.542  | 8.196   |
| CLAM (5 cm)           | 17.578              | 16.337 | 17.492  | 11.181             | 11.268 | 11.184  | 7.861  | 7.249  | 7.820   |

## CHAPTER 5

### CONCLUSIONS AND FUTURE WORK

#### 5.1. CONCLUSIONS

In a fusion reactor, the FW suffers the highest degree of material damage in the top part of the blanket facing directly into the fusion chamber. In addition, maintenance and replacement of FW are very difficult and costly and require long plant shutdown times. Additionally, in FW, low levels of DPA and gas productions (He and H) are essential for continuous, long plant uptimes. Therefore, in this study, the modeling of a magnetic fusion reactor was determined based on the blanket parameters of ITER. Stainless Steel (SS 316 LN-IG), Oxide Dispersion Strengthened Steel Alloy (PM2000 ODS) and China low activation martensitic steel (CLAM) were used as a First Wall (FW) materials. Fluorides family molten salt materials (FLiBe, FLiNaBe, FLiPb) and Lithium oxide (LiO<sub>2</sub>) were considered as a coolant and the tritium production material in the blanket, respectively. The effects of changing first wall materials and their thickness on the reactor were investigated DPA and gas production in the first wall and TBR in the coolant zone and the tritium breeding zone.

Neutronic calculations were performed by the Monte Carlo methods using the widely applied 3D particle transport code MCNP uses the latest built-in continuous energy nuclear and the activity cross section data libraries, the Evaluated Nuclear Data File (ENDF) system (ENDF/B-V and ENDF/B-VI) and CLAW-IV. The most recent version MCNP was applied successfully for the evaluation of the neutronic parameters. This can mean that it is generally considered a good predictor of processes and systems.

The main results can be summarized as follows:

- The lead-containing coolant increases higher efficiency tritium breeding and the contribution of the lead-containing (Pb) coolant (FLiPb) to the total TBR clearly shows a sharp increase in tritium production in the Tritium Cultivation Zone.
- Both M factor and TBR are the highest in the FLiPb coolant, additionally M and TBR values decrease as the thickness for first wall materials increases.
- The first wall is 2 cm for all materials, the TBR value produced in the coolant zone is sufficient and the best performance was obtained for 1 cm first wall material Stainless Steel (PM2000 ODS).
- The lead containing FLiPb coolant is the highest DPA values for the first wall materials.
- Since Fe and Cr elements are in the highest content of all the first wall materials, one can say that the DPA damages of the first wall materials are approximately similar.
- Higher H-production than He-production was obtained for the investigated FW structures.
- Since all the hydrogen isotopes will diffuse out of the metallic lattice or form metal hybrids, H-production values were not taken into consideration in this study.
- The lowest He-production values were obtained for FLiPb coolant, the highest He-production values were obtained almost same for FLiBe and FLiNaBe coolants.
- He-production was considered as the factor determining the replacement of FW material due to He/DPA ratio.

- The replacement periods were obtained between 6 years and 11 years for He-production limit.

## **5.2. FUTURE WORKS**

The following research points should be considered during the future studies.

- Molten Salt studies are a key technology for both Fusion reactors and GEN-IV reactors. Especially neutronic studies on these subjects should be continued.
- Structure material technology is very important in all nuclear fields. For this reason, neutronic studies on material damage should be carried out on new steel structure materials.

## REFERENCES

1. Comprehensive Energy Systems, Volume 1, Energy Fundamental 5, Chapter 1,20 Nuclear Energy (1).
2. Internet: <https://www.energy.gov/science/doe-explainsnuclear-fusion-reactions>.
3. Principles of Fusion Energy By (author): A A Harms (McMaster University, Canada) D R Kingdon (McMaster University, Canada) K F Schoepf (University of Innsbruck, Austria) and G H Miley (University of Illinois, Urbana-Champaign, USA) (<https://doi.org/10.1142/4447> | June 2000).
4. El-Guebaly, L.A., Fifty years of magnetic fusion research (1958-2008): Brief historical overview and discussion of future trends. *Energies* 3, 1067–1086 (2010).
5. ITER, EDA. "Documentation Series No. 24 ITER Technical Basis", IAEA, Vienna - pub. [iaea.org/MTCDC/publications/PDF/ITER-EDA-DS-24.pdf](http://iaea.org/MTCDC/publications/PDF/ITER-EDA-DS-24.pdf) (2002).
6. Sawan, M.E., Abdou, M.A., Physics and technology conditions for attaining tritium self-sufficiency for the DT fuel cycle. *Fusion Engineering and Design*. 81, 1131–1144, (2006).
7. Şahin, H.M., Monte Carlo calculation of radiation damage in first wall of an experimental hybrid reactor. *Annals of Nuclear Energy*, 34, 861–870, (2007).
8. Soltani, B., Habibi, M., Tritium breeding ratio calculation for ITER tokamak using developed helium cooled pebble bed blanket (HCPB). *Journal of Fusion Energy* 34, 604–607, (2015).
9. Hernández, F.A., Pereslavitsev, P., First principles review of options for tritium breeder and neutron multiplier materials for breeding blankets in fusion reactors. *Fusion Engineering and Design*. 137, 243–256, (2018).
10. Tobita, Kenji, et al. Water-cooled solid breeding blanket for DEMO. Paper Presented at the 18th International Toki Conference (ITC18), February, Development of Physics and Technology of Stellarators/Heliotrons en route to DEMO, (Toki, Japan 2009)
11. Şahin, S., Şahinaslan, A., Kaya, M., Neutronic calculations for a magnetic fusion energy reactor with liquid protection for the first wall. *Fusion Technology*, 34-2, 95–108, (1998).
12. Yalçın, S., Übeyli, M., Acir, A., Neutronic analysis of a high-power density hybrid reactor using innovative coolants. *Sadhana*, 30, 585–600, (2005).

13. Şahin, S., Şahin, H.M., Acir, A., LIFE hybrid reactor as reactor grade plutonium burner, *Energy Convers. Manag.* 63, 44-50, (2012).
14. Sawan, M., Tritium Breeding Potential of Lithium-Tin. APEX Proj. Meet. (1998).
15. Youssef, M.Z., Sawan, M.E., Sze, D.K., The breeding potential of “Flinabe” and comparison to “Flibe” in “CliFF” high power density concept. *Fusion Engineering and Design*. 61–62, 497–503, (2002).
16. Şahin, H.M., Tunç, G., Şahin, N., Investigation of tritium breeding ratio using different coolant material in a fusion-fission hybrid reactor. *International Journal of Hydrogen Energy*, 41, 7069–7075, (2016).
17. Şahin, H.M., et al., Monte Carlo calculation for various enrichment lithium coolant using different data libraries in a hybrid reactor. *Energy Conversion and Management*, 49, 1960–1965 (2008).
18. Übeyli, M., On the tritium breeding capability of Flibe, Flinabe, and  $\text{Li}_{20}\text{Sn}_{80}$  in a fusion-fission (hybrid) reactor. *Journal of Fusion Energy* 22, 51–57, (2003).
19. Şahin, S., et al., Study on the fusion reactor performance with different materials and nuclear waste actinides. *International Journal of Energy Research*. 1–16, (2020).
20. Catalán, J.P., et al., Neutronic analysis of a dual He/LiPb coolant breeding blanket for DEMO. *Fusion Engineering and Design* 86, 2293–2296, (2011).
21. Wang, S., et al., Comparative analysis of the efficiency of a  $\text{CO}_2$ -cooled and a He-cooled pebble bed breeding blanket for the EU DEMO fusion reactor. *Fusion Engineering and Design*. 138, 32–40, (2019).
22. Tillack, M. S., et al. "Technology readiness of helium as a fusion power core coolant." *Center for Energy Research* (2014).
23. Romatoski, R.R. Hu, L.W. Fluoride salt coolant properties for nuclear reactor applications: A review, *Annals of Nuclear Energy*, Volume 109, 635-647, (2017).
24. R´emi Boullon, Jean-Charles Jaboulay, Julien Aubert, “Molten salt breeding blanket: Investigations and proposals of pre-conceptual design options for testing in DEMO”, *Fusion Engineering and Design*, 171, 112707, (2021).
25. Cadwallader, L.C., Qualitative reliability issues for in-vessel solid and liquid wall fusion designs. *Fusion Technology*. 39, 991–995, (2001).
26. Dobran, F., Fusion energy conversion in magnetically confined plasma reactors. *Progress in Nuclear Energy* 60, 89–116, (2012).
27. Tunç, G., Şahin, H.M., Şahin, S., Evaluation of the radiation damage parameters of ODS steel alloys in the first wall of deuterium-tritium fusion-fission (hybrid) reactors. *International Journal of Energy Research*, 42, 198-206, (2018).

28. Muroga, T., Vanadium Alloys for Fusion Blanket Applications. *Materials Transactions*, 46(3), 405–411, (2005).
29. Q. Huang, et al., Progress in development of China Low Activation Martensitic steel for fusion application, *Journal of Nuclear Materials* 367–370, 142–146, (2007).
30. Garry McCracken, Peter Stott, Chapter 13 - Fusion Power Plants, ed. by Garry McCracken, Peter Stott, *Fusion (Second Edition)*, (Academic Press, 2013), p. 165-187
31. Şahin, H.M., Tunç, G., Karakoç, A., Omar, Melood Mohamad. Neutronic study on the effect of first wall material thickness on tritium production and material damage in a fusion reactor. *Nuclear Science and Techniques*, 33,43 (2022).
32. Ioki, K., et al. "Design of the ITER vacuum vessel", *Fusion Engineering and Design*, 27, 39-51, (1995).
33. Araujo, Arione, et al. "Flux and dose rate evaluation of ITER system using MCNP-a preliminary simulation", *Brazilian Journal of Physics*, vol. 40, no. 1, (March 2010).
34. X-5 Monte Carlo Team, "MCNP - Version 5, Vol. I: Overview and Theory", LA-UR-03-1987 (2003).
35. Garber, D., C. Dunford, and S. Pearlstein. Data Formats and procedures for the evaluated nuclear data file, ENDF. No. BNL-NCS-50496; ENDF-102. Brookhaven National Lab., Upton, NY, USA, (1975).
36. Battat, M. E. ANS-6.1. 1 Working group, "American National Standard Neutron and Gamma-Ray Flux-to-Dose Rate factors,". ANSI/ANS-6.1. 1-1977, American Nuclear Society, LaGrange Park, Illinois, USA, (1977).
37. Kinsey, R. Data formats and procedures for the evaluated nuclear data file, ENDF. No. BNL-NCS--50496 (ED. 2). Brookhaven National Lab., (1979).
38. Rose, P. F. ENDF-201: ENDF/B-VI summary documentation. No. BNL-NCS-17541; ENDF-201. Brookhaven National Lab., Upton, NY (United States), (1991).
39. Al-Kusayer, T. A., S. Şahin, and A. Drira. "CLAW-IV coupled 30 neutrons, 12 gamma-ray group cross sections with retrieval programs for radiation transport calculations." Radiation Shielding Information Center, RSIC Newsletter, Oak Ridge National Laboratory 4 (1988).
40. G. Tunc, Ph.D. Dissertation (Department of Energy Systems Engineering Gazi University, 2017), (in Turkish)
41. Şahin, S., Şahin, H.M., Tunç, T., Monte Carlo analysis of LWR spent fuel transmutation in a fusion-fission hybrid reactor system, *Nuclear Engineering and Technology*, Volume 50, Issue 8, Pages 1339-1348, (2018)

42. Rubel, M., Fusion Neutrons: Tritium Breeding and Impact on Wall Materials and Components of Diagnostic Systems, *Journal of Fusion Energy*, 38:315–329, (2019).
43. Internet: Nuclear Data Center at Korea Atomic Energy Research Institute (KAERI). Nuclear Data Plotter, <https://atom.kaeri.re.kr/nuchart/plotEvaf.jsp>; [accessed October 19, 2021].
44. Moir, et al., HYLIFE-II. a molten-salt inertial fusion energy power plant designing. Final Report. *Fusion Technology*, 26. p. 5. (1994).
45. Smith, Dale L., et al. Overview of the blanket comparison and selection study. *Fusion Technology* 8.1 P1: 10-44 (1985).
46. Blink, James A., et al. High-yield lithium-injection fusion-energy (HYLIFE) reactor. No. UCRL-53559. Lawrence Livermore National Lab., CA, USA, (1985).
47. Perlado, M., et al. Radiation Damage in Structural Materials, Energy from Inertial Fusion, International Atomic Energy Agency, 272, Vienna, (1995).
48. Herman, M., et al. "Evaluation of neutron reactions on iron isotopes for CIELO and ENDF/B-VIII. 0." *Nuclear Data Sheets* 148: 214-253, (2018).
49. Duderstadt, James J., and Gregory A. Moses. Inertial confinement fusion. (John Wiley & Sons, 1982).
50. Hofman, E.A. et al., Radioactive waste disposal characteristics of candidate tokamak demonstration reactors. *Fusion Technology*. 31, 35, (1997).
51. Youssef, M.Z., Wong, C., Neutronics performance of high temperature refractory alloy helium-cooled blankets for fusion application. *Fusion Engineering and Design*. 49-50, 727, (2000).
52. Standard, A. S. T. M. "Standard Practice for Characterizing Neutron Exposure in Iron and Low Alloy Steels in Terms of Displacements Per Atom (dpa)." (2001).

## **RESUME**

I joined Gharyan High School in 1981-1982 and obtained a secondary certificate in the 84-1985 academic year. I continued my university studies at the Technical College of Civil Aviation & meteorology, Department of Mechanical power Engineering, and graduated from College 88-1989. I spent four years in a research center as a maintenance engineer. I left the center in 1994 and started working at the Higher Institute of Science & Technology and was sent to study for a master's degree in Poland in 2002 and obtained a master's degree from Warsaw University of Technology in 2005. I worked as a director of the institute and a lecturer until i joined Karabuk University, Department of Energy Systems, in February 2018.